SUPPLEMENT SERIES

Astron. Astrophys. Suppl. Ser. **125,** 263-287 (1997)

Multiwavelength optical observations of chromospherically active binary systems

I. Simultaneous Hα, Na I D_1, D_2, and He I D_3 observations*

D. Montes, M.J. Fernández-Figueroa, E. De Castro, and J. Sanz-Forcada

Departamento de Astrofísica, Facultad de Físicas, Universidad Complutense de Madrid, E-28040 Madrid, Spain
e-mail: dmg@ucmast.fis.ucm.es

Received October 14; accepted December 23, 1996

Abstract. This is the first paper of a series aimed at studying the chromosphere of active binary systems using the information provided for several optical spectroscopic features. Simultaneous Hα, Na I D_1, D_2, and He I D_3 spectroscopic observations are reported here for 18 systems. The chromospheric contribution in these lines have been determined using the spectral subtraction technique. Very broad wings have been found in the subtracted Hα profile of some of the more active stars. These profiles are well matched using a two-components Gaussian fit (narrow and broad) and the broad component could be interpreted as arising from microflaring. Prominence-like extended material have been detected in a near-eclipse Hα observation of the system AR Lac. The excess emission found in the Na I D_1 and D_2 lines by application of the spectral subtraction technique and the behaviour of the Hα line in the corresponding simultaneous observations indicate that the filling-in of the core of these lines is a chromospheric activity indicator. For giant stars of the sample the He I D_3 line has been detected in absorption in the subtracted spectra. An optical flare has been detected in UX Ari and II Peg through the presence of the He I D_3 in emission in coincidence with the enhancement of the Hα emission.

Key words: stars: activity — stars: binaries: close — stars: chromospheres — stars: flare — stars: late-type

1. Introduction

The chromospherically active binaries are detached binary systems with cool components characterized by strong chromospheric, transition region, and coronal activity. The RS CVn systems have at least one cool evolved component whereas both components of the BY Dra binaries are main sequence stars (Fekel et al. 1986).

In this series of papers we try to study the chromosphere of this kind of extremely active stars using the information provided by several optical spectroscopic features that could be used as chromospheric activity indicators. The simultaneous observations of different lines, that are formed at different height in the chromosphere (from the region of temperature minimum to the higher chromosphere), are of special interest for stellar activity studies since they provide very useful information about this stellar region. Ideally, simultaneous observations should be performed at all wavelengths in order to develop a coherent 3-D atmosphere model. In practice, simultaneous observations of several activity indicators are rare and tend to focus on the same small number of extremely active systems.

The best way to obtain the active-chromosphere contribution to some spectral line in the chromospherically active binaries is to subtract the underlying photospheric contribution using the spectral subtraction technique (subtraction of a synthesized stellar spectrum constructed from artificially rotationally broadened, radial-velocity shifted, and weighted spectra of inactive stars chosen to match the spectral types and luminosity classes of both components of the active system under consideration).

The emissions in the Ca II H & K resonance lines are the most widely used optical indicators of chromospheric activity, since their source functions are collisionally controlled and represent an extremely important cooling mechanism. In chromospheric active binaries the

Send offprint requests to: D. Montes

* Based on observations made with the Isaac Newton telescope operated on the island of La Palma by the Royal Greenwich Observatory at the Spanish Observatorio del Roque de Los Muchachos of the Instituto de Astrofísica de Canarias.

subtraction of the photospheric flux in this spectral region has been recently applied using the spectral subtraction (see Montes et al. 1995c, 1996a and references therein).

The Hα line is also an important chromospheric activity indicator, but it is only in emission above the continuum in very active stars, and in less active star only a filled-in absorption line is observed. So, to infer chromospheric activity level the spectral subtraction is needed (see Montes et al. 1994; 1995a,b,d, and references therein; Lázaro & Arévalo 1997). A similar behaviour is observed in the other Balmer lines (Hall & Ramsey 1992; Montes et al. 1995d).

Recently, the spectral subtraction technique has been used in other lines as the Ca II IRT, Mg I b, Na I D_1, D_2, and He I D_3 lines (Gunn & Doyle 1997; Gunn et al. 1997). The Ca II IRT lines are formed deeper in the atmosphere and are thus sensitive probes of the temperature minimum region. The Na I D_1, D_2 lines are collision dominated and are good indicators of changes in the lower chromosphere. The Mg I b triplet lines are formed in the lower chromosphere and the region of temperature minimum and they are good diagnostics of photospheric activity (Basri et al. 1989). The He I D_3 line has been largely ignored as activity indicator; however it could be a valuable probe of stellar activity and the observation of this line in emission supports the detection of flare like events (Zirin 1988).

In this first paper we focus our study on the analysis of the extensively used Hα chromospheric activity indicator together with simultaneous observations of the less studied He I D_3 and Na I D_1, D_2 spectral features in a sample of 18 northern active binary systems selected from "A Catalog of Chromospherically Active Binary Stars (second edition)" (Strassmeier et al. 1993, hereafter CABS). By using the spectral subtraction technique, we have determined the excess emission in these lines and we have computed absolute chromospheric fluxes in Hα. The primary aim of this study is analyse in detail the excess Hα emission and to study the subtracted Hα line profile, especially in some extremely active stars which exhibit broad wings. Moreover, we try to understand the behaviour of the He I D_3 and Na I D_1, D_2 lines as chromospheric activity indicators taking into account the advantage that we simultaneously know the behaviour of the chromospheric excess Hα emission in these systems. In forthcoming papers we will analyze in detail several optical spectroscopic features using echelle spectroscopy in order to determine the effects of stellar activity on spectral lines originating at different heights in the chromosphere. Another of our goals is to obtain information about the presence of extended matter (prominence-like structures) in the chromospheric active binaries using simultaneous Hα and Hβ observations at near-eclipse orbital phases.

In Sect. 2 we give the details of our observations and data reduction. In Sect. 3 we describe the individual results of Hα, Na I D_1, D_2, and He I D_3 line observations of our sample. Finally in Sect. 4 we discuss our results.

2. Observations and data reduction

Observations in the Hα and Na I D_1, D_2, He I D_3 line regions have been obtained during three nights (1995 September 13-15) with the Isaac Newton Telescope (INT) at the Observatorio del Roque de Los Muchachos (La Palma, Spain) using the Intermediate Dispersion Spectrograph (IDS) with grating H1800V, camera 500 and a 1024×1024 pixel TEK3 CCD as detector. The reciprocal dispersion achieved is 0.24 Å/pixel which yields a spectral resolution of 0.48 Å and a useful wavelength range of 250 Å centered at 6563 Å (Hα) and 5876 Å (HeI D_3) respectively.

The spectra have been extracted using the standard reduction procedures in the IRAF package (bias subtraction, flat-field division, and optimal extraction of the spectra). The wavelength calibration was obtained by taking spectra of a Cu-Ar lamp. Finally, the spectra have been normalized by a polynomial fit to the observed continuum.

In Table 1 we give the observing log. For each star we list the date, UT, orbital phase (φ) and signal to noise ratio (S/N) obtained for each observation in both spectral regions. Where appropriate, we also give the reference of our previous observation of these systems in the Hα and Ca II H & K lines.

In Table 2 we show the HD number, name and the adopted stellar parameters (from CABS or the references given in the table) for the 18 chromospherically active binary systems selected.

We have obtained the chromospheric contribution in Hα Na I D_1, D_2, and He I D_3 lines using the spectral subtraction technique described in detail by Montes et al. (1995a,c).

The synthesized spectra were constructed using artificially rotationally broadened, radial-velocity shifted, and weighted spectra of inactive stars chosen to match the spectral types and luminosity classes of both components of the active system under consideration. The reference stars used have been observed in this campaign and previous observational seasons with similar spectral resolution (see the spectral library of Montes et al. 1997).

In some case, the difference spectrum obtained appears noisier than expected from the observation S/N ratio (≈ 300) due to small differences in spectral type between active and reference star, or to non appropriate evaluation of the rotational broadening and/or of the Doppler shift. In addition, in some spectra telluric lines also appear in the difference spectrum. This noise in the the difference spectrum have been evaluated as the mean standard deviation (σ) in the regions outside the chromospheric features. We have obtained values of σ in the range $0.01 - 0.03$ which could be important in low active star but in the more active stars the errors in the excess Hα EW are small. We have considered as a clear detection of excess emission or absorption in Hα, Na I D_1, D_2, and

Table 1. Hα and Na I D_1, D_2, He I D_3 Observing log, and previous Hα and Ca II H & K observations

Name	Hα line region				Na I D_1, D_2, He I D_3 line region				Previous obs.	
	Date	UT	φ	S/N	Date	UT	φ	S/N	Hα	Ca II
BD Cet	1995/09/15	00:43	0.569	330	1995/09/15	01:03	0.569	361	-	95c, 96a
AY Cet	1995/09/15	02:03	0.797	385	1995/09/15	02:20	0.797	398	-	95c, 96a
AR Psc	1995/09/13	01:48	0.373	387	1995/09/13	01:27	0.372	141	94, 95a	94, 96a
''	1995/09/14	01:42	0.443	361	1995/09/14	02:00	0.443	369	-	-
''	1995/09/15	03:55	0.519	392	1995/09/15	04:23	0.520	399	-	-
''	1995/09/15	05:34	0.524	305	1995/09/15	05:28	0.523	359	-	-
HD 12545	1995/09/15	02:59	0.401	354	1995/09/15	02:25	0.400	361	-	95c, 96a
UX Ari	1995/09/13	02:08	0.419	346					95b	95c, 96a
''	1995/09/13	05:08	0.438	202	1995/09/13	04:52	0.437	494	-	-
''	1995/09/14	02:24	0.576	276	1995/09/14	02:09	0.574	293	-	-
''	1995/09/15	03:09	0.736	352	1995/09/15	03:32	0.739	410	-	-
V711 Tau	1995/09/13	05:15	0.922	360	1995/09/13	05:36	0.927	370	94, 95a	94, 96a
''	1995/09/14	04:19	0.261	374	1995/09/14	04:35	0.265	423	-	-
''	1995/09/14	05:35	0.280	332	1995/09/14	05:50	0.283	386	-	-
''	1995/09/15	03:50	0.606	342	1995/09/15	03:44	0.605	332	-	-
''	1995/09/15	06:11	0.641	314	1995/09/15	06:05	0.639	326	-	-
V833 Tau	1995/09/13	06:13	0.762	184	1995/09/15	05:47	0.752	325	95b	-
''	1995/09/14	06:07	0.319	424	1995/09/14	05:55	0.314	417	-	-
''	1995/09/15	04:56	0.851	394	1995/09/15	05:18	0.859	322	-	-
V1149 Ori	1995/09/15	06:17	0.439	311	1995/09/15	06:29	0.439	335	95b	95c, 96a
MM Her	1995/09/12	20:56	0.498	274	1995/09/12	21:31	0.501	329	94, 95a	94, 96a
''	1995/09/13	22:06	0.630	332	1995/09/13	20:45	0.623	384	-	-
''	1995/09/14	20:09	0.745	257	1995/09/14	20:41	0.748	314	-	-
V815 Her	1995/09/12	20:43	0.978	360	1995/09/12	20:21	0.970	341	94, 95a	94, 96a
''	1995/09/13	20:15	0.520	375	1995/09/13	20:22	0.523	341	-	-
''	1995/09/14	21:24	0.099	354	1995/09/14	21:44	0.107	394	-	-
BY Dra	1995/09/13	22:58	0.684	387	1995/09/13	23:15	0.686	372	-	94, 96a
''	1995/09/14	21:56	0.839	398	1995/09/14	21:05	0.838	404	-	-
V775 Her	1995/09/14	22:03	0.394	342	1995/09/14	21:53	0.392	373	94, 95a	94,96a
V478 Lyr	1995/09/14	22:14	0.953	326	1995/09/14	22:33	0.959	412	-	94, 96a
HK Lac	1995/09/12	22:56	0.067	343	1995/09/12	22:42	0.067	357	94, 95a	94, 96a
''	1995/09/13	00:42	0.070	130	1995/09/13	00:25	0.070	193	-	-
''	1995/09/13	23:44	0.110	346	1995/09/13	23:58	0.110	343	-	-
''	1995/09/14	01:37	0.113	332	1995/09/14	01:21	0.113	264	-	-
''	1995/09/14	22:53	0.149	321	1995/09/14	23:09	0.149	339	-	-
''	1995/09/15	01:26	0.153	329	1995/09/15	01:21	0.153	358	-	-
AR Lac	1995/09/12	22:16	0.405	360	1995/09/12	21:57	0.399	421	94, 95a	94, 96a
''	1995/09/13	23:39	0.939	346	1995/09/13	23:23	0.933	415	-	-
''	1995/09/14	22:49	0.425	339	1995/09/14	22:42	0.423	407	-	-
KZ And	1995/09/14	23:29	0.145	336	1995/09/14	23:51	0.150	367	-	94, 95c, 96a
KT Peg	1995/09/13	00:07	0.693	221	1995/09/13	00:13	0.694	271	-	95c, 96a
"	1995/09/15	01:19	0.024	313	1995/09/15	01:13	0.023	368	-	-
II Peg	1995/09/12	23.02	0.575	300	1995/09/12	23:23	0.577	298	-	-
''	1995/09/13	00:58	0.587	138	1995/09/13	01:18	0.589	240	-	-
''	1995/09/14	00:57	0.735	265	1995/09/14	01:14	0.737	324	-	-
''	1995/09/14	03:07	0.749	315	1995/09/14	02:51	0.747	328	-	-
''	1995/09/14	05:00	0.760	266	1995/09/14	05:16	0.762	263	-	-
''	1995/09/14	23:22	0.874	318	1995/09/14	23:15	0.873	324	-	-
''	1995/09/15	01:56	0.890	332	1995/09/15	01:49	0.889	352	-	-
''	1995/09/15	04:38	0.907	298	1995/09/15	04:31	0.906	311	-	-

94: Fernández-Figueroa et al. (1994), 95a: Montes et al. (1995a), 95b: Montes et al. (1995b), 95c: Montes et al. (1995c), 96a: Montes et al. (1996a).

He I D_3 only when these features in the difference spectrum are larger than 3 σ.

Table 3 gives the Hα line parameters, measured in the observed and subtracted spectra of the sample. Column (2) of this Table gives the orbital phase (φ) for each spectrum, and in Col. (3), H and C mean emission belonging to hot and cool component respectively, and T means that at these phases the spectral features cannot be deblended. Column (4) gives the contributions for the hot and cool component to the total continuum ($S_{\rm H}$ and $S_{\rm C}$). Column (5) describes the observed Hα profile, i.e. if the line is in absorption (A) in emission (E) or totally filled by emission (F). Columns (6), (7), (8) give the following parameters measured in the observed spectrum: the full width at half maximum ($W_{\rm obs}$); the residual intensity, $R_{\rm c}$; and the Hα core flux, $F(1.7$ Å$)$, measured as the residual area below

Table 2. Stellar parameters

HD	Name	T_{sp}	SB	R ($R_\odot$)	d (pc)	$V-R$	P_{orb} (days)	P_{rot} (days)	$V\sin i$ (km s^{-1})
1833	BD Cet	K1III	1	≥10	71	0.81	35.1	34.46	15
7672	AY Cet	WD/G5III	1	0.012/15	66.7	0.69	56.824	77.22	4
8357	AR Psc	G7V/K1IV[1]	2	/≥1.5	17	0.74[1]	14.30226[1]	12.245	6.5/3.5[1]
12545	XX Tri	K0III	1	≥8	310	[0.62]	23.9824	24.3	17
21242	UX Ari	G5V/K0IV	2	0.93/≥4.7	50	0.70/0.54	6.43791	≈P_{orb}	6/37
22468	V711 Tau	G5IV/K1IV	2	1.3/3.9	36	0.62/0.75	2.83774	2.841	13/38
283750	V833 Tau	dK5e	1	≥0.22	16.7	0.69	1.7878	1.797	6.3
37824	V1149 Ori	K1III	1	≥11	[164]	0.90	53.58	54.1	11
341475	MM Her	G2/K0IV	2	1.58/2.83	190	[/0.64]	7.960322	7.936	10/18
166181	V815 Her	G5V/[M1-2V]	1	0.93:/	31	0.54	1.8098368	1.8	27/
234677	BY Dra	K4V/K7.5V	2	1.2-1.4/	15.6	1.10	5.975112	3.827	8.0/7.4
175742	V775 Her	K0V/[K5-M2V]	1	0.85/	24	0.80	2.879395	2.898	15/
178450	V478 Lyr	G8V/[dK-dM]	1	≥0.9	26	0.65	2.130514	2.185	21/
209813	HK Lac	F1V/K0III	1	-	150	0.75	24.4284	24.4284	/15
210334	AR Lac	G2IV/K0IV	2	1.8/3.1	47	0.77	1.98322195	1.98322195	46/81
218738	KZ And	dK2/dK2	2	≥0.74/	[≈23]	[0.74/0.74]	3.032867	3.03	12.3/11.6
222317	KT Peg	G5V/K6V	2	0.93/0.72	25	[0.54/]	6.20199	6.092	8/5
224085	II Peg	K2-3V-IV	1	2.2	29.4	0.89	6.724183	6.718	21

[1] Parameters from Fekel (1996).

the central 1.7 Å passband. The last four Columns give he following parameters measured in the subtracted spectrum: the full width at half maximum (W_{sub}), the peak emission intensity (I), the excess Hα emission equivalent width (EW(Hα)), and absolute fluxes at the stellar surface logF_S(Hα) obtained with the calibration of Pasquini & Pallavicini (1991) as a function of ($V-R$), very similar values of F_S(Hα) are obtained using the more recently calibration of Hall (1996) as a function of ($V-R$) and ($B-V$). For a more detailed description of the parameters given in this table see our previous study of the excess Hα emission in active binaries (Montes et al. 1995a).

In Table 4 we list the parameters (I, $FWHM$, EW) of the broad and narrow components used in the two Gaussian components fit to the Hα subtracted emission profile, which we have performed in the stars that present broad wings. See the comments for each individual star in Sect. 3 and the interpretation of these components given in Sect. 4.

3. Individual results

In the following we describe the Hα, Na I D_1, D_2, and He I D_3 spectra of the stars of this sample. The line profiles of each chromospherically active binary system are displayed in Figs. 1 to 19 The name of the star, the orbital phase, and the expected positions of the features for the hot (H) and cool (C) components are given in each figure. For each system we plot the observed spectrum (solid-line), the synthesized spectrum (dashed-line), the subtracted spectrum, additively offset for better display (dotted line) and the Gaussian fit to the subtracted spectrum (dotted-dashed line).

3.1. BD Cet (HD 1833)

Single-lined spectroscopic binary classified as K1III + F by Bidelman & MacConnell (1973). It presents strong Ca II H & K emission lines centered at the absorption line (Montes et al. 1995c) and the Hα line as moderate absorption (Fekel et al. 1986).

We have obtained one spectrum of this system at the orbital phase 0.569 (see Fig. 1). The Hα subtracted spectrum shows a weak excess emission. In the Na I line region no detectable filling-in of the D_1 and D_2 lines is present. A clear absorption in the He I D_3 line appears in the subtracted spectrum. In both spectral regions the spectrum is matched using a K2III as reference star.

3.2. AY Cet (39 Cet, HD 7672, HR 373)

AY Cet is a single-lined binary composed of a spotted G5III primary and a white dwarf secondary. It presents strong Ca II H & K emission lines (Montes et al. 1995c) and a filled in absorption Hα line (Fekel et al. 1986; Strassmeier et al. 1990).

We present here one observation of this system at the orbital phase 0.797 (see Fig. 2). In the Hα line region we have used a G8III reference star to perform the spectral subtraction and the subtracted spectrum obtained shows a weak excess emission. No detectable filling-in of the Na I D_1 and D_2 lines has been found, however, a weak absorption in the He I D_3 line appears in the subtracted spectrum.

3.3. AR Psc (HD 8357)

This extremely active RS Cvn system is a double-lined spectroscopic binary consisting of a K1IV primary and

Table 3. Hα line measures in the observed and subtracted spectrum

				Observed Hα Spectrum				Subtracted Hα Spectrum			
Name	φ	E	$S_{\rm H}/S_{\rm C}$	Hα	$W_{\rm obs}$ (Å)	$R_{\rm c}$	F(1.7 Å)	$W_{\rm sub}$ (Å)	I	EW (Å)	$\log F_{\rm S}$
BD Cet	0.569	-	-	A	1.80	0.452	0.928	0.82	0.221	0.193	5.75
AY Cet	0.797	-	-	A	1.62	0.446	0.940	1.08	0.214	0.245	6.02
AR Psc	0.373	-	0.20/0.80	E	-	1.065	1.715	1.47	0.599	1.071	6.58
"	0.443	-	0.20/0.80	E	-	1.063	1.680	1.61	0.653	1.403	6.70
"	0.519	-	0.20/0.80	E	-	1.059	1.736	1.46	0.676	1.211	6.64
"	0.524	-	0.20/0.80	E	-	1.070	1.755	1.47	0.687	1.263	6.66
XX Tri	0.401	-	-	E	2.68	1.387	2.301	1.80	1.089	2.599	6.92
UX Ari	0.419	C	0.30/0.70	E	1.26	1.225	1.966	1.89	0.722	1.798	6.85
"	0.438	C	0.30/0.70	E	1.07	1.101	1.799	1.82	0.626	1.405	6.74
"	0.576	C	0.30/0.70	E	1.41	1.159	1.818	1.83	0.609	1.476	6.76
"	0.736	C	0.30/0.70	E	3.17	1.533	2.504	2.51	0.996	3.286	7.11
V711 Tau	0.922	C	0.16/0.84	E	3.36	1.315	2.084	2.48	0.837	2.710	6.96
"	0.261	C	0.16/0.84	E	3.63	1.264	2.095	2.26	0.759	2.524	6.93
"	0.280	C	0.16/0.84	E	3.51	1.255	2.081	2.24	0.763	2.421	6.92
"	0.606	C	0.16/0.84	E	2.93	1.342	2.185	2.20	0.842	2.641	6.95
"	0.641	C	0.16/0.84	E	2.88	1.328	2.164	2.24	0.812	2.382	6.91
V833 Tau	0.762	-	-	E	1.61	1.087	1.808	1.37	0.754	1.101	6.37
"	0.319	-	-	E	-	1.078	1.738	1.35	0.709	1.018	6.34
"	0.851	-	-	E	1.56	1.085	1.790	1.35	0.745	1.070	6.36
V1149 Ori	0.439	-	-	A	2.00	0.476	0.953	0.91	0.269	0.259	5.75
MM Her	0.498	C	0.59/0.41	A	1.65	0.561	1.118	1.42	0.320	0.590	6.38
"	0.630	H	0.50	A	-	0.588	1.101	-	0.000	0.000	0.00
		C	0.50	A	-	0.846	1.490	1.46	0.302	0.541	6.34
"	0.745	H	0.50	A	-	0.603	1.134	-	0.000	0.000	0.00
		C	0.50	A	-	0.831	1.476	1.41	0.270	0.494	6.30
V815 Her	0.978	H	-	F	-	0.878	1.508	1.75	0.535	1.279	6.95
"	0.520	H	-	A	-	0.739	1.314	1.65	0.396	0.875	6.79
"	0.099	H	-	A	-	0.787	1.390	1.80	0.445	1.095	6.89
BY Dra	0.684	T	0.70/0.30	E	1.39	1.202	1.919			1.357	
		H	0.70	E				1.36	0.540	0.780	6.20
		C	0.30	E				1.70	0.319	0.577	5.73
"	0.839	T	0.70/0.30	E	1.70	1.270	2.039			1.455	
		H	0.70	E				1.38	0.548	0.803	6.22
		C	0.30	E				1.89	0.324	0.652	5.78
V775 Her	0.394	H	-	E	-	1.044	1.719	1.39	0.745	1.103	6.51
		C	-	E	-	1.027	1.690	1.02	0.138	0.149	-
V478 Lyr	0.953	H	-	A	3.36	0.763	1.353	1.53	0.446	0.727	6.55
HK Lac	0.067	C	-	A	1.66	0.611	1.178	1.31	0.366	0.765	6.43
"	0.070	C	-	A	1.75	0.610	1.170				
"	0.110	C	-	A	1.61	0.657	1.243	1.32	0.411	0.887	6.49
"	0.113	C	-	A	1.61	0.647	1.237				
"	0.149	C	-	A	1.61	0.664	1.257	1.37	0.420	0.929	6.51
"	0.153	C	-	A	1.57	0.661	1.244				
AR Lac	0.405	H	0.36	A	-	0.787	1.401	1.92	0.083	0.169	5.98
		C	0.64	A	-	0.774	1.335	2.037	0.114	0.248	6.00
"	0.425	H	0.37	A	-	0.696	1.241	1.44	0.062	0.095	5.73
		C	0.63	A	-	0.675	1.167	0.92	0.018	0.018	4.86
"	0.939	H	0.27	A	-	-	-	-	-	-	-
		C	0.73	A	-	-	-	-	0.050	0.104	5.59
KZ And	0.145	1	0.58	A	1.81	0.780	1.404	1.06	0.209	0.237	5.94
		2	0.42	A	-	0.884	1.517	1.22	0.207	0.269	5.99
KT Peg	0.693	C	0.95/0.05	A	1.85	0.349	0.786	-	0.000	0.000	0.00
"	0.024	C	0.95/0.05	A	1.77	0.354	0.792	-	0.000	0.000	0.00
II Peg	0.575	-	-	E	1.69	1.456	2.316	1.62	1.134	2.127	6.66
"	0.587	-	-	E	1.69	1.456	2.302	1.62	1.135	2.146	6.66
"	0.735	-	-	E	2.04	1.407	2.311	1.69	1.102	2.362	6.70
"	0.749	-	-	E	2.02	1.393	2.295	1.66	1.087	2.486	6.72
"	0.760	-	-	E	2.63	1.505	2.484	1.80	1.198	3.692	6.88
"	0.874	-	-	E	1.87	1.279	2.102	1.57	0.956	1.963	6.62
"	0.890	-	-	E	1.91	1.267	2.084	1.57	0.942	1.972	6.62
"	0.907	-	-	E	1.85	1.288	2.096	1.66	0.959	1.961	6.62

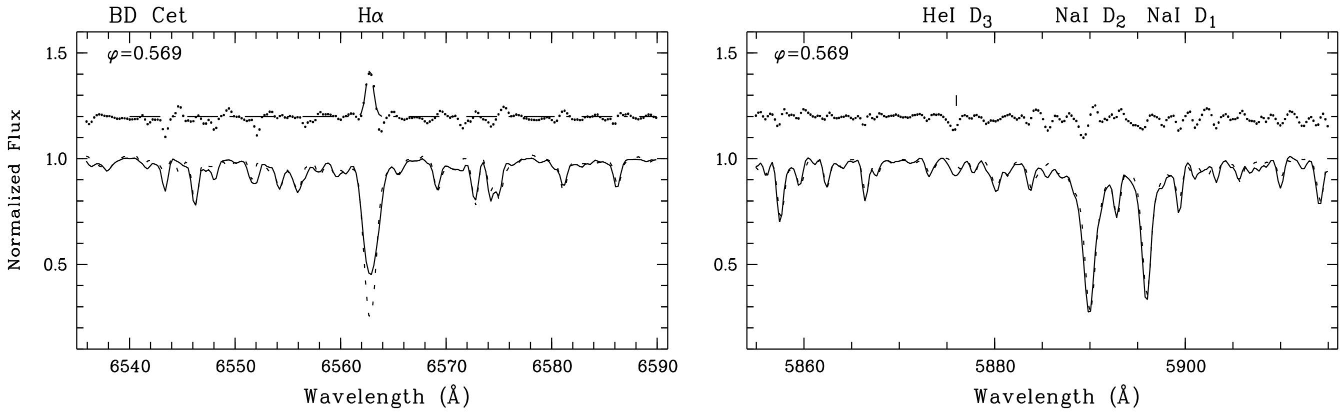

Fig. 1. Hα, Na I D_1, D_2, and He I D_3 spectra of BD Cet

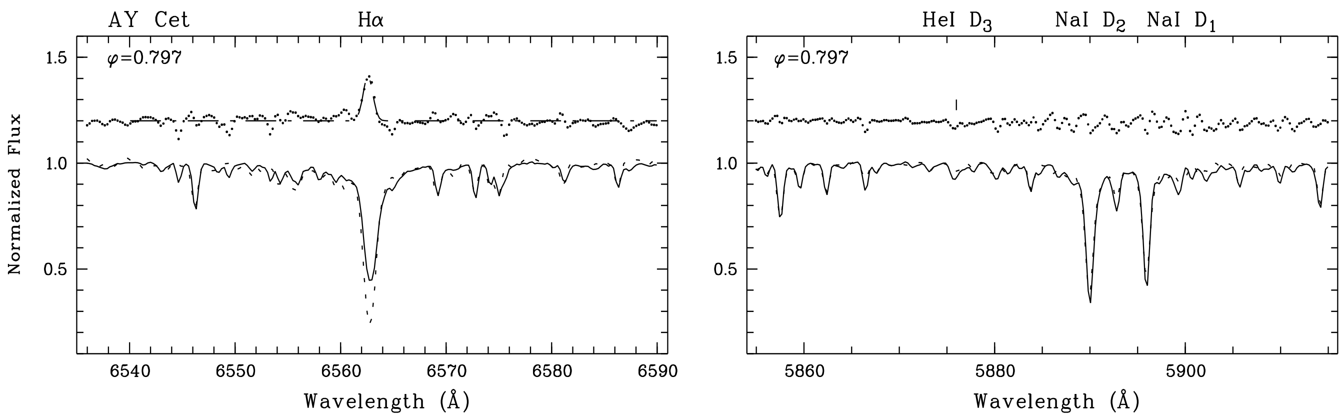

Fig. 2. Hα, Na I D_1, D_2, and He I D_3 spectra of AY Cet

a G7V secondary (Fekel 1996). In our previous observations of this system we have found strong Ca II H & K and $H\epsilon$ emissions from the cool component (FFMCC), the Hα line of the active component in emission above the continuum (FFMCC and Montes et al. 1995a, b) and an important filling-in by chromospheric emission in the $H\beta$ line (Montes et al. 1995d).

Now we have analysed four spectra of this system in both spectral regions at the orbital phases from 0.37 to 0.52 (see Fig. 3). The Hα line of the active component appears in emission above the continuum, with a profile that changes with the orbital phase owing to the different amounts of overlapping with the absorption of the other component. By subtracting the synthesized spectrum, constructed with G6IV and K0IV reference stars and a relative contribution of 0.2/0.8 we have found a large excess Hα emission which is well matched using a two-components Gaussian fit. In the Na I D_1 and D_2 lines an important excess emission is present in the subtracted spectra, however, the He I D_3 line does not appear in absorption.

3.4. HD 12545 (XX Tri, BD +34 363)

This extremely active RS CVn binary is a single-lined spectroscopic binary of spectral type K0III. It has very strong Ca II H & K and Hϵ emission lines and the Hα line in emission above the continuum (Strassmeier et al. 1990; Bopp et al. 1993; Montes et al. 1995c). This system shows the largest amplitude of light variation from spots yet recorded (Hampton et al. 1996).

Our observed Hα spectrum at the orbital phase 0.401 (Fig. 4) shows a strong and very broad Hα emission above the continuum. The synthesized spectrum has been constructed with a reference star of spectral type K0III obtaining a satisfactory fit. The subtracted spectrum exhibits an asymmetric profile that is not well matched using a Gaussian fit, therefore we fit the profile by means two Gaussian components. In the Na I line region a clear excess emission in the D_1 and D_2 lines is present, in agreement with the strong activity of this system. The behaviour of the He I D_3 line is not clear in this spectrum, but a weak absorption seems to appear.

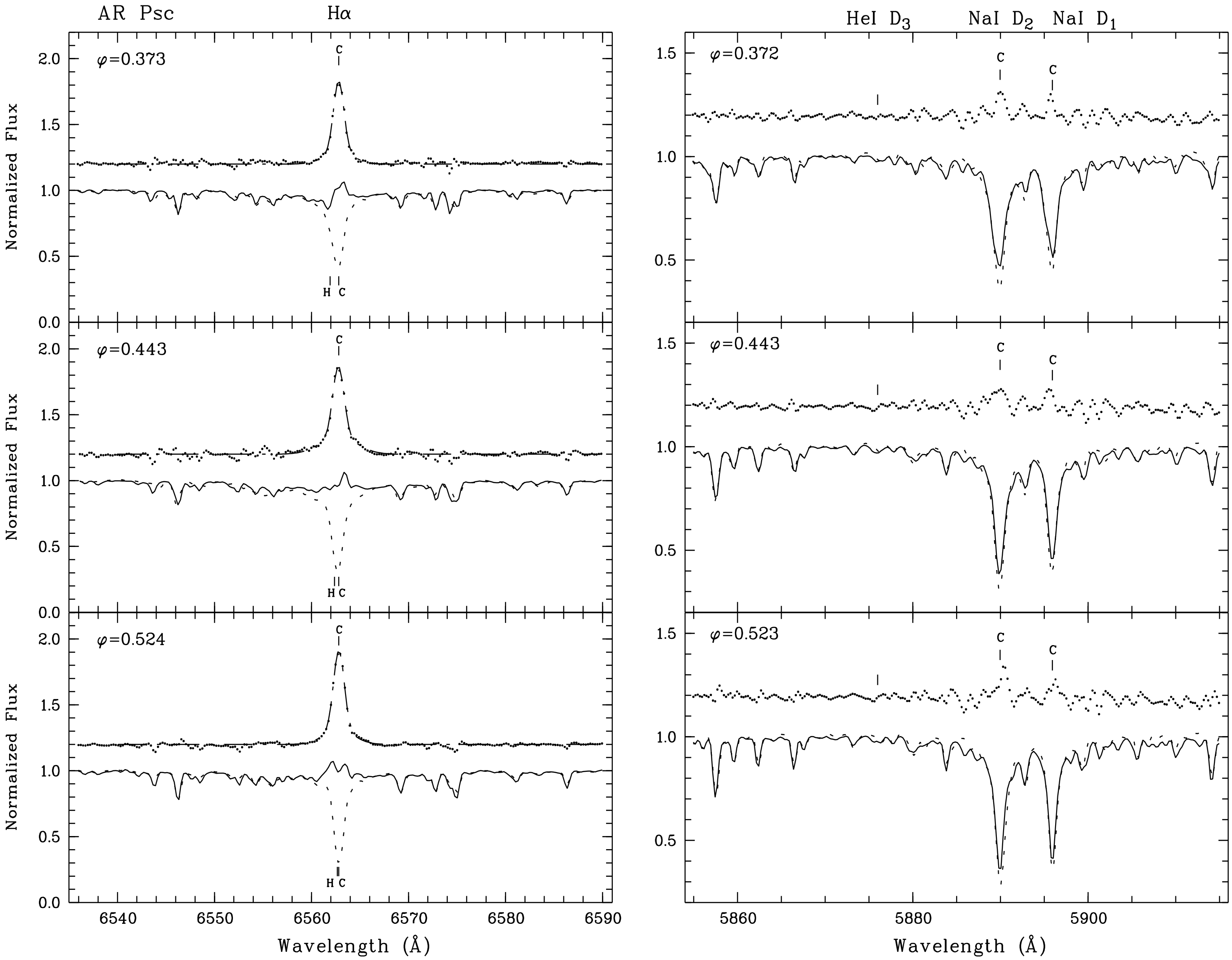

Fig. 3. Hα, Na I D_1, D_2, and He I D_3 spectra of AR Psc

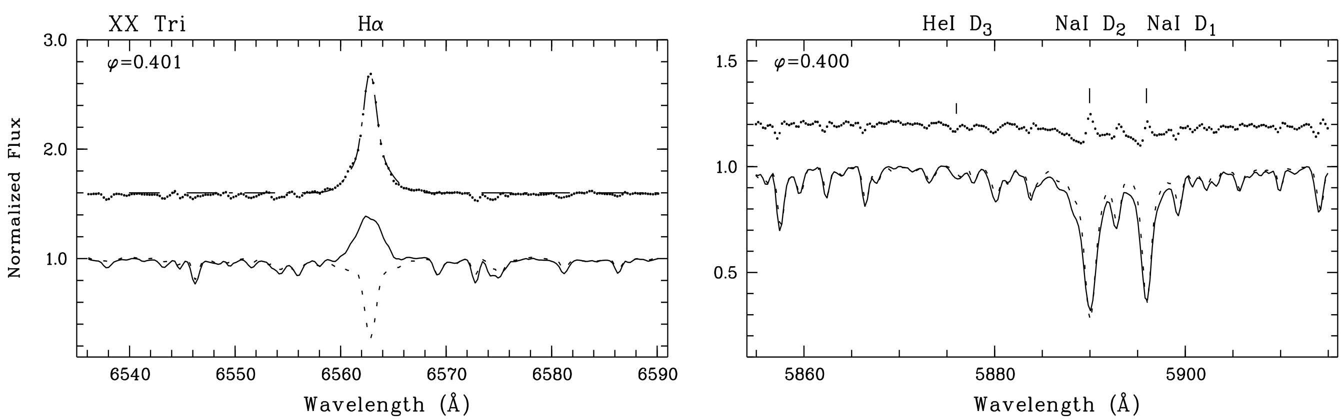

Fig. 4. Hα, Na I D_1, D_2, and He I D_3 spectra of XX Tri (HD 12545)

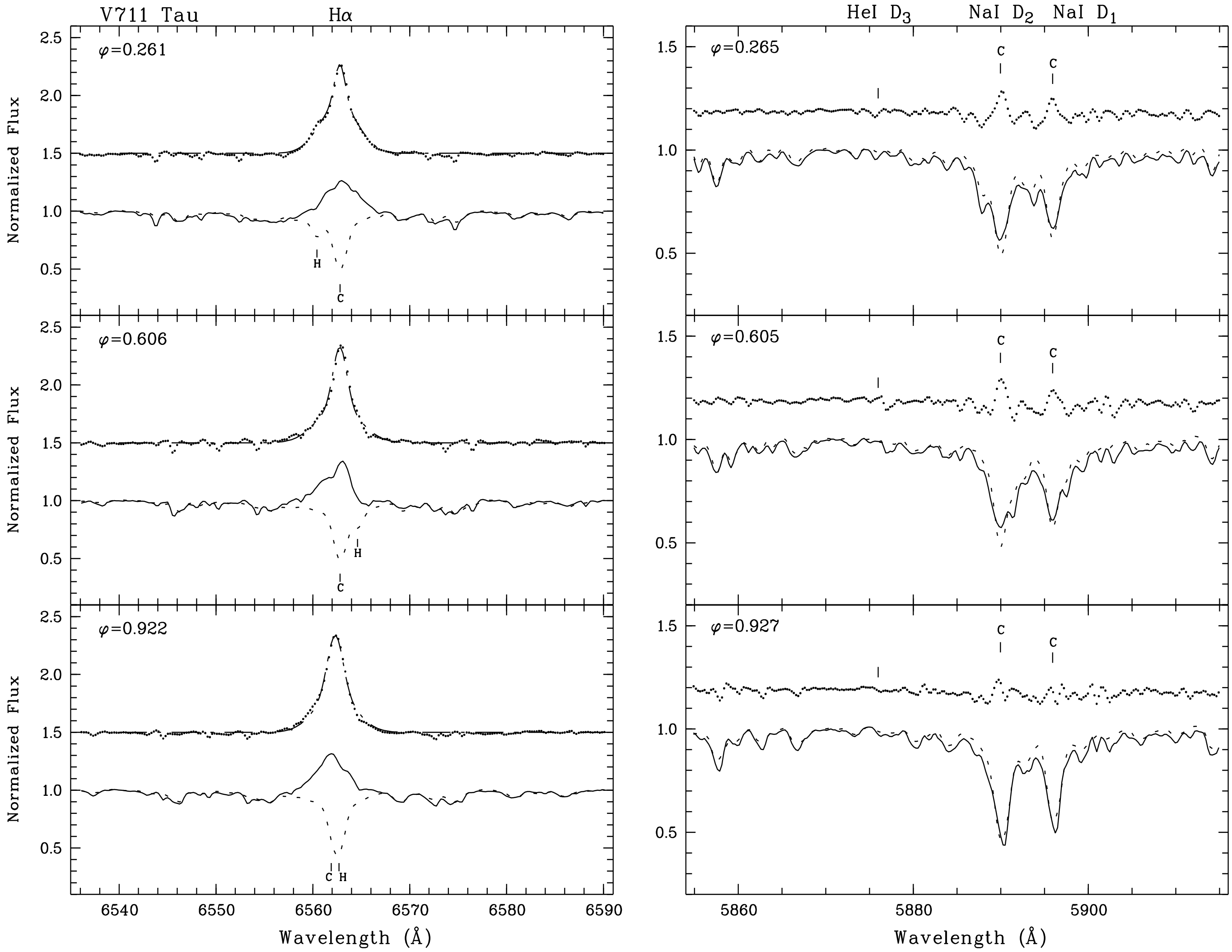

Fig. 5. Hα, Na I D_1, D_2, and He I D_3 spectra of V711 Tau

3.5. UX Ari (HD 21242)

The description of the simultaneous Hα, Na I D_1, D_2, and He I D_3 observations and the detection of a flare on this system can be found in Montes et al. (1996b).

3.6. V711 Tau (HR 1099, HD 22468)

V711 Tau, one of the most active of the RS CVn binaries, is a double-lined spectroscopic binary whose components have spectral types G5IV and K1IV. Our Ca II H & K analysis of this system (FFMCC) showed that both components present emissions. The cool component is the more active star in the system, and also presents the Hϵ line in emission. This system shows the Hα line in emission above the continuum and the spectral subtraction (Montes et al. 1995b) reveals that the K1 star is responsible for most of the excess Hα emission. Recently UV observations obtained with the HST's GHRS (Wood et al. 1996; Dempsey et al. 1996b,c) indicate that the transition region lines of V711 Tau are emitted almost entirely by the K1 star, and the G star contributes 14% to the chromospheric Mg II h & k lines flux.

We report here five new observations of this systems in the Hα line region at the orbital phases 0.92, 0.26, 0.28, 0.61 and 0.64 (1995 September 13-15) (see Fig. 5) that confirm the results obtained in our previous observations taken in 1988, 1986 and 1992. The Hα subtracted profiles presents at all the epochs broad wings and are not well matched using a single-Gaussian fit. These profiles have therefore been fitted using two Gaussian components. The parameters of the broad and narrow components used in the two-Gaussian fit are given in Table 4 and the corresponding profiles are plotted in Fig. 6. In contrast to the behaviour found in other systems in which we have used a two-Gaussian fit, the broad component of V711 Tau dominates the line profile (the average contribution of the broad component to the total Hα *EW* is 77%, whereas in other stars the contribution ranges between 35% and

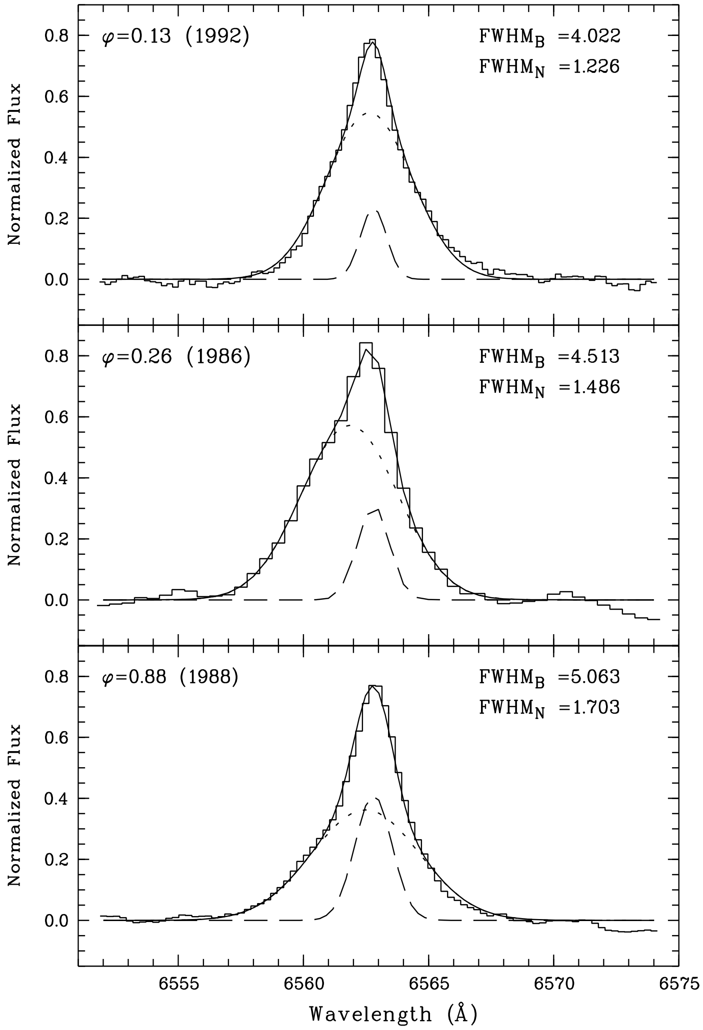

Fig. 6. Subtracted Hα profiles of V711 Tau at different epochs and orbital phases (line in histogram from). We have superposed the two Gaussian components fit (solid-line). The sort-dashed-line represents the broad component and the large-dashed-line the narrow one

63%). Wood et al. (1996) and Dempsey et al. (1996c) also found this behaviour in the broad component of the chromospheric and transition region lines of V711 Tau in comparison with the broad components found in the less active stars AU Mic and Capella.

In Fig. 6 we can also see that, the contribution of the broad component is larger at orbital phases near 0.2 (80 − 87%) than at larger orbital phases (63 − 72%) and this behaviour remains at different epochs (see Fig. 6). These changes indicate not only that the broad component is the result of microflaring in the chromosphere, as in other stars, but that large and long-lived chromospheric flares, that take place in this system (Dempsey et al. 1996c), could also produced enhanced emission in the extended line wings.

Variable excess emission appears in the Na I D_1 and D_2 lines of the corresponding subtracted spectra, however, no detectable absorption is observed in the He I D_3 line.

3.7. V833 Tau (HD 283750)

V833 Tau is a BY Dra system (dK5e) and one of the hottest known flare stars. In our previous observations of this system we have found a moderate Hα emission above the continuum that presents a variable little central self-reversal (Montes et al. 1995a,b) and a strong Hβ excess emission (Montes et al. 1995d).

We analyse here three new observations of this systems in the Hα line region at orbital phases 0.762, 0.319, and 0.851 (Fig. 7) that confirm the behaviour previously noted. The self-reversal feature changes its wavelength-position across the emission Hα line profile, however, it

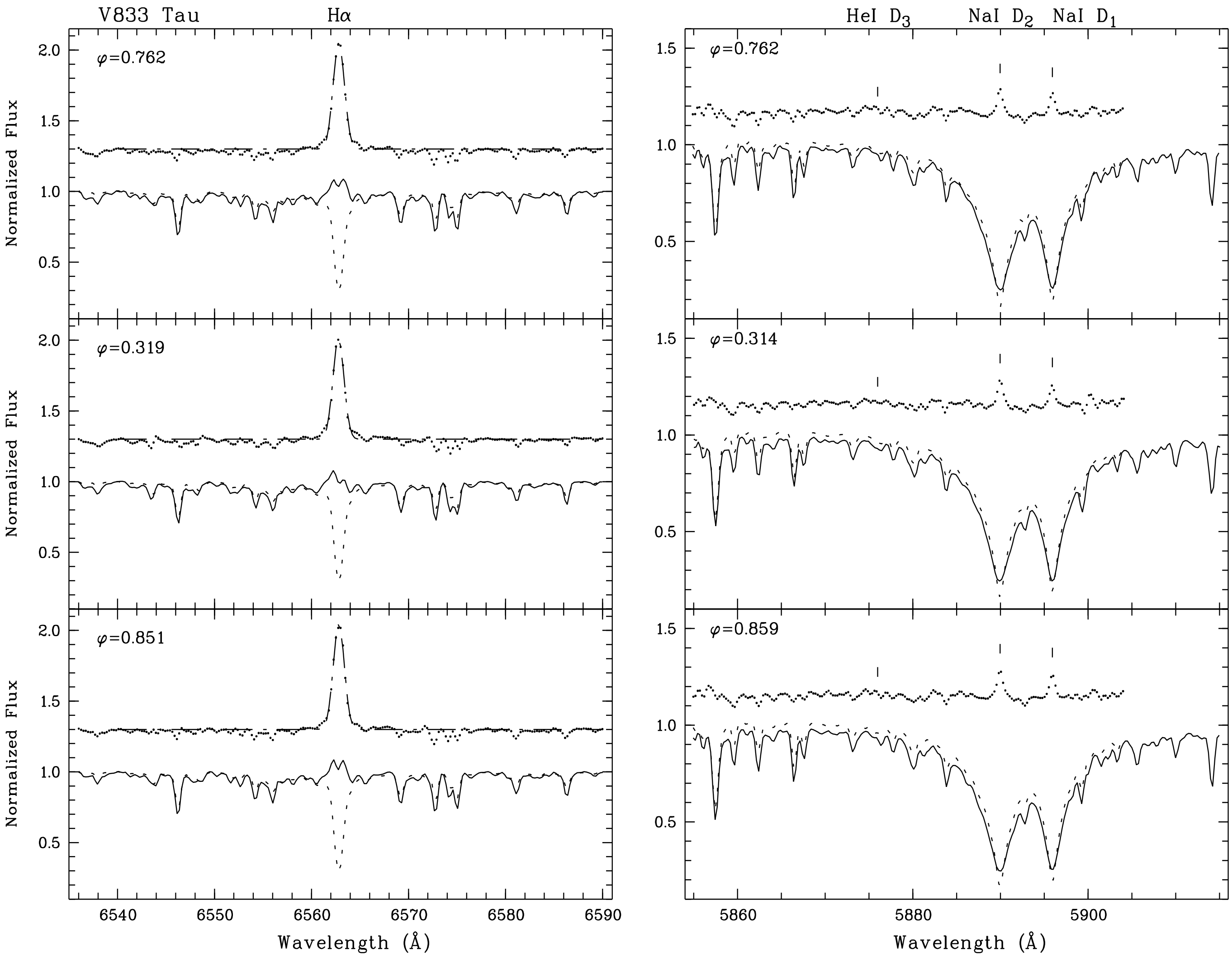

Fig. 7. Hα, Na I D_1, D_2, and He I D_3 spectra of V833 Tau

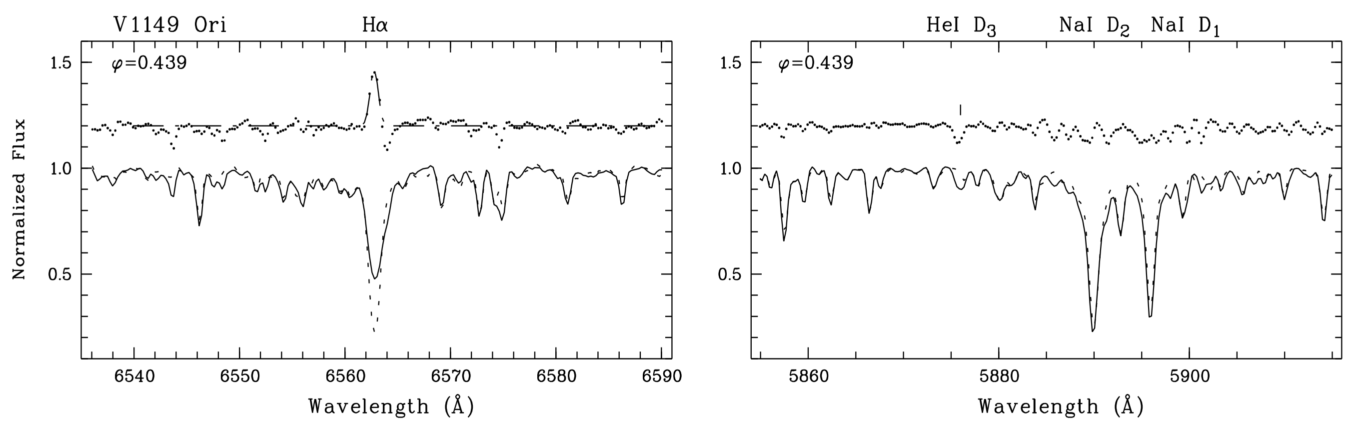

Fig. 8. Hα, Na I D_1, D_2, and He I D_3 spectra of V1149 Ori

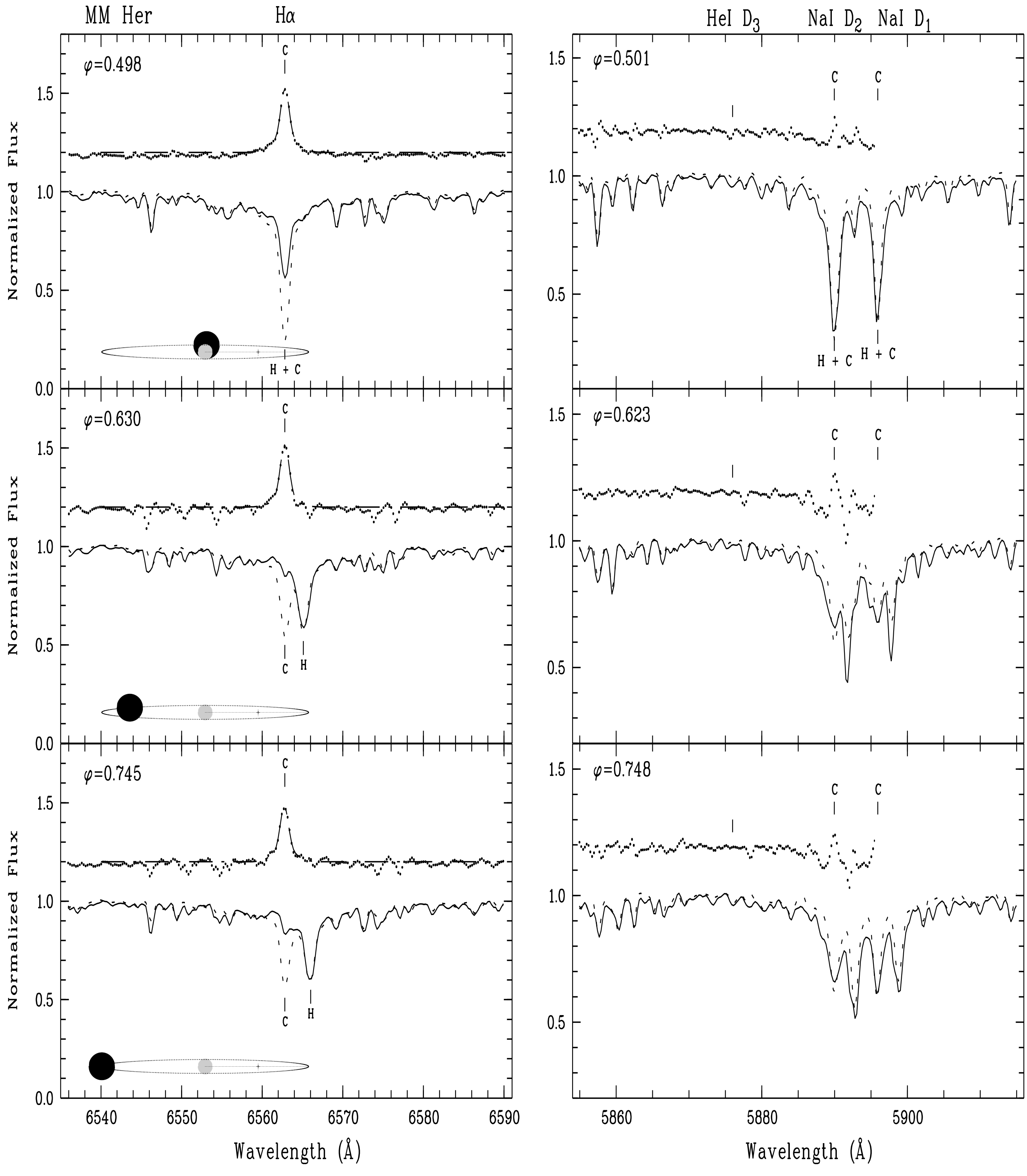

Fig. 9. Hα, Na I D_1, D_2, and He I D_3 spectra of MM Her

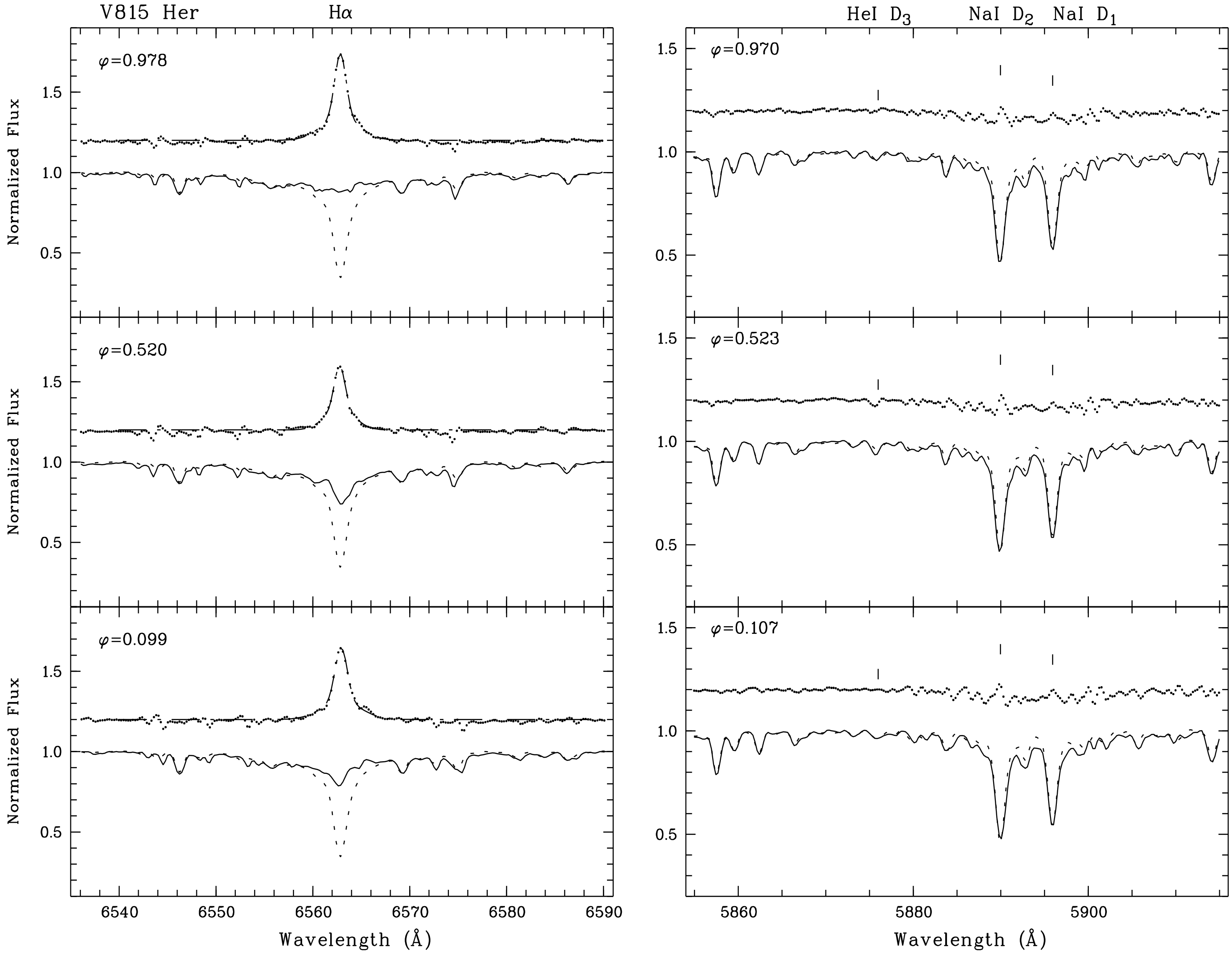

Fig. 10. Hα, Na I D_1, D_2, and He I D_3 spectra of V815 Her

appears always centered with the corresponding Hα absorption line of the synthesized spectrum.

The Na I D_1 and D_2 lines exhibit very broad wings in the observed spectra, as correspond to a star of spectral type as later as K5. Although the observed and synthesized spectra are not well matches, due to problems in the normalization, a clear excess emission in the D_1 and D_2 lines can be seen in the subtracted spectra. The He I D_3 line is not detected in this star.

3.8. V1149 Ori (HD 37824)

A single-lined spectroscopic binary classified as K1III. Our previous observations reveal a clear excess Hα emission (Montes et al. 1995a,b), strong Ca II H & K and Hϵ emission lines (Montes et al. 1995c).

We present here one spectrum at the orbital phase 0.439 (see Fig. 8). The difference with respect to a K0III reference star reveals a lower excess Hα emission than the obtained in our previous observations in 1992 (Montes et al. 1995a). The narrow absorption that appears in the red wing of the excess Hα emission in the subtracted spectra could be attributed to a telluric line.

The spectral subtraction reveals that this star has no measurable filling-in of the Na I D_1 and D_2 lines. However, a clear absorption in the He I D_3 line appears in the subtracted spectrum.

3.9. MM Her (HD 341475)

Double-lined spectroscopic binary (G2/K0IV) with partial eclipses. This system has Ca II H & K emission lines from both components and excess Hα emission from the cool component (FFMCC, Montes et al. 1995a).

We have obtained three new spectra (Fig. 9) of this system in the Hα and Na I D_1 and D_2 line regions at orbital phases 0.498, 0.630, and 0.745. At phase 0.498 the hot component hides a 0.30 fraction of the cool one, (see

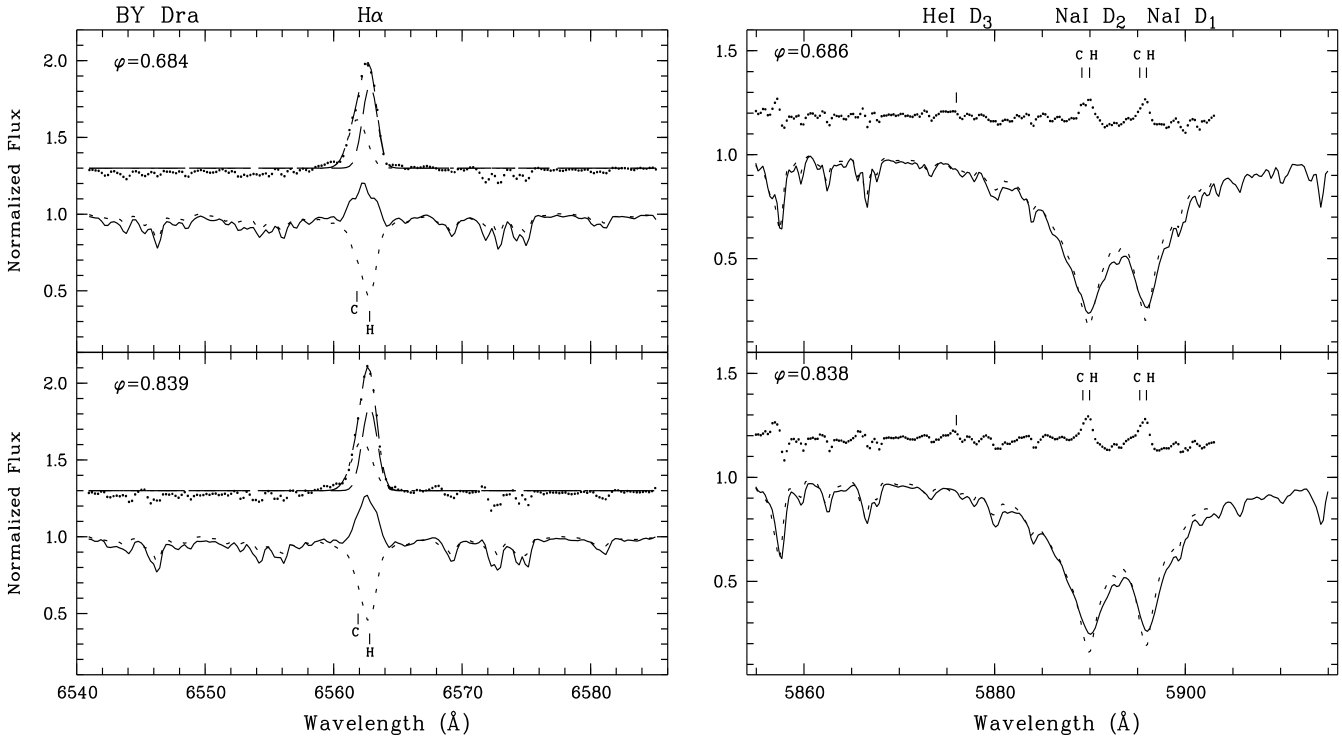

Fig. 11. Hα, Na I D_1, D_2, and He I D_3 spectra of BY Dra. In the subtracted Hα spectra we have superposed the Gaussian fit used to deblend the contribution of the hot and cool components

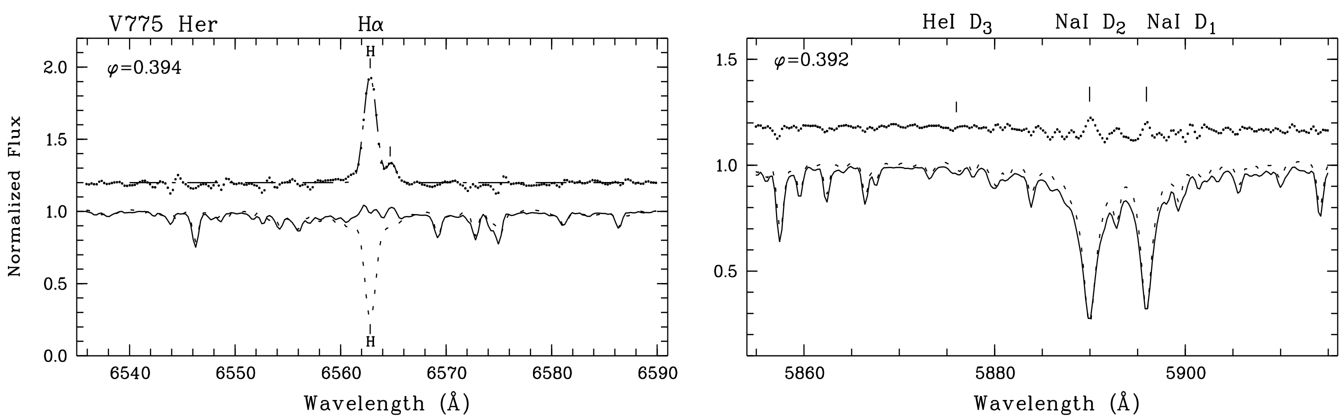

Fig. 12. Hα, Na I D_1, D_2, and He I D_3 spectra of V775 Her

the diagram of Fig. 9) and the absorption lines from both components appear overlapped in the observed spectrum. However, at phases 0.630 and 0.745 there is not eclipse and the lines are clearly wavelength-shifted. The more intense Hα absorption observed in these spectra corresponds to the hot component and the less intense and blue-shifted absorption corresponds to the cool one. The spectral subtraction, using G2IV and K0IV as reference stars and a relative contribution of 0.5/0.5, indicates that the excess Hα emission arises only from the cool component. The excess Hα emission line profiles obtained are well matched using a two-component Gaussian fit.

In the subtracted spectra of the Na I D_1 and D_2 lines region we can also see an excess emission in these lines from the cool component. The narrow absorption that appears near the position of the hot component could be due to deficient sky correction in these spectra. The He I D_3 line is not present.

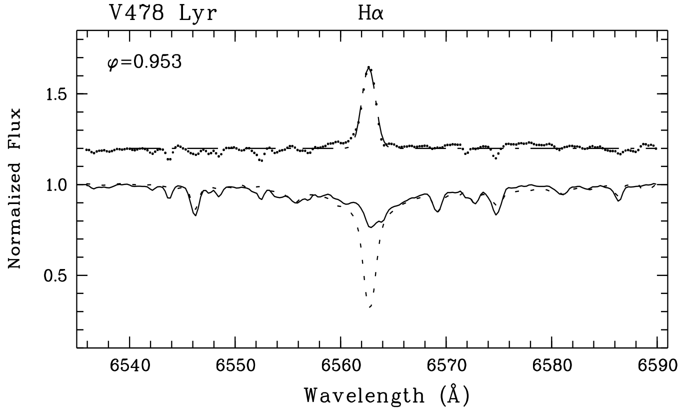

Fig. 13. Hα, Na I D_1, D_2, and He I D_3 spectra of V478 Lyr

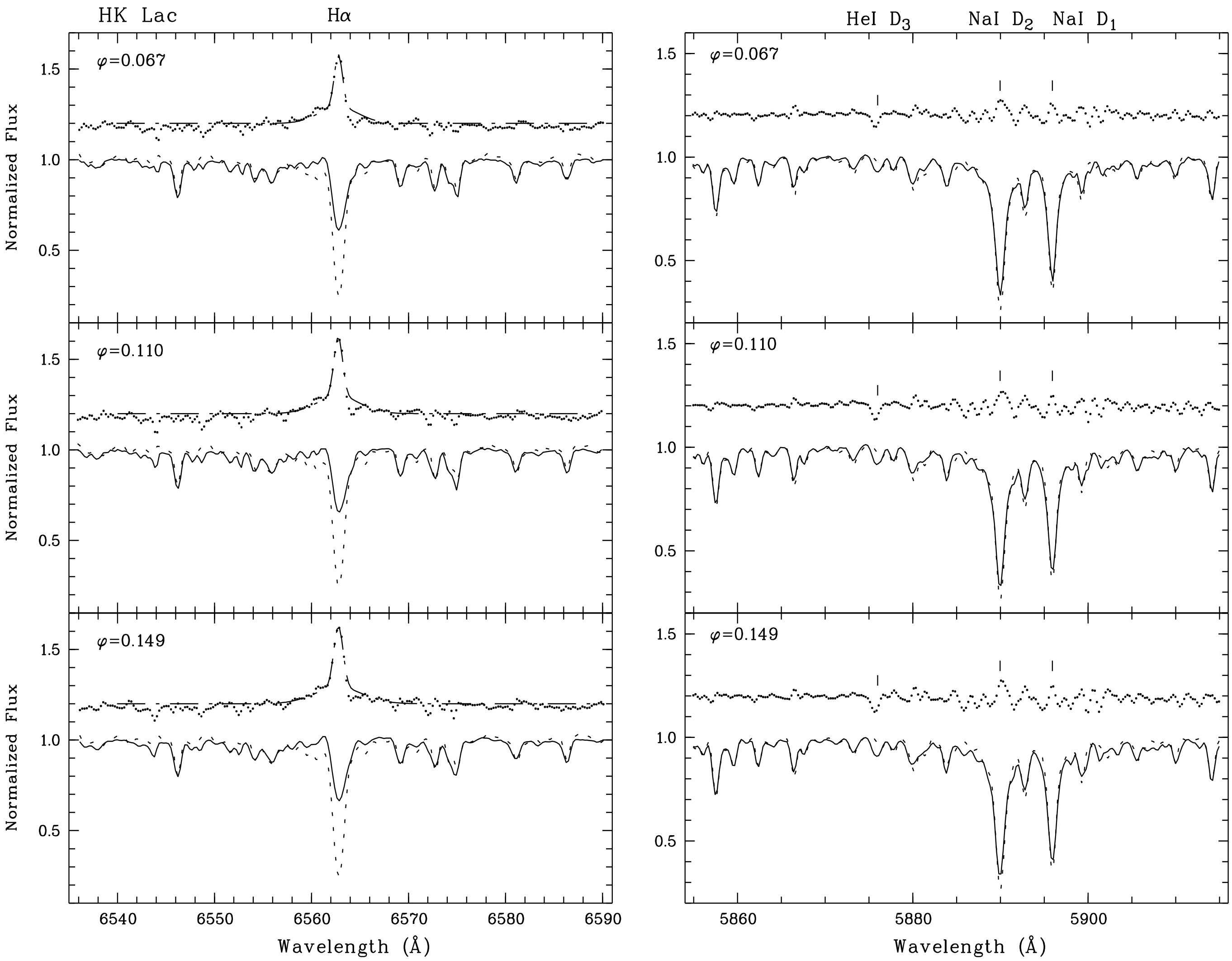

Fig. 14. Hα, Na I D_1, D_2, and He I D_3 spectra of HK Lac

3.10. V815 Her (HD 166181)

Single-lined spectroscopic binary. Our previous Ca II H & K and Hα observations (FFMCC, Montes et al. 1995a) indicate that the hot star is the active component. Multiwavelength observations of this system have been recently reported by Dempsey et al. (1996a).

We have taken three spectra of this system at orbital phases 0.978, 0.520, 0.099 (see Fig. 10). In the Hα line region the spectra show a filling-in absorption line with noticeable night to night changes. The excess Hα emission obtained with the spectral subtraction of a G5 V reference star is larger at the orbital phases near to 0.0. The subtracted Hα profile presents broad wings and is well matched using a fit with two Gaussian components (narrow and broad). The narrow component is more important when the excess Hα emission is larger (see Table 4).

A small filling-in is observed in the Na I D_1 and D_2 lines at the three orbital phases, and only at phase 0.523 absorption in detected in the He I D_3 line.

3.11. BY Dra (HD 234677)

The prototype of the BY Dra stars. Our previous Ca II H & K observations of this system (FFMCC) clearly show that both components are active with the hot component having the stronger Ca II emission. The two components also show Hϵ in emission.

We present in this paper simultaneous Hα and Na I D_1 and D_2 observations of this system at orbital phases 0.684 and 0.839 (see Fig. 11). These spectra show strong Hα emission above the continuum and the Na I D_1 and D_2 lines with very broad wings corresponding to the later spectral type of the components of this system (K4V/K7.5V).

By applying the spectral subtraction technique we have obtained an asymmetric excess Hα emission line profile which has contributions from both components. A two-Gaussian fit has been used to deblend the contribution of the hot and cool components to the line profile. This fit reveals that the hot component have the stronger excess Hα emission *EW* in agreement with the behaviour observed by us in the Ca II H & K lines.

The subtracted spectra in the Na I D_1 and D_2 line region reveal that the excess emission in these lines also arises from both components. The He I D_3 line is not detected in these spectra.

3.12. V775 Her (HD 175742)

Single-lined spectroscopic binary (K0V/[K5 − M2V]) with strong Ca II H & K emission lines from the hot component (FFMCC). The Hα feature may change from a weak absorption feature to emission above the continuum on times scales of hours (Xuefu & Huisong 1984).

In our Hα spectrum at the orbital phase 0.394 (Fig. 12) we can see the Hα line of the hot component totally filled-in by emission and a small emission bump red-shifted in relation to the absorption lines. By subtracting the synthesized spectrum, constructed with a K0IV reference star, we have obtained a strong excess Hα emission coming from the hot component and a small excess emission, red-shifted 1.9 Å with respect to the emission of the hot component. This small excess perhaps could be attributed to the cooler star of the system, whose assumed spectral type is K5 − M2V and whose contribution to the observed spectra is negligible.

In the Na I lines region the spectral subtraction points out a filling-in of the D_1 and D_2 lines and not detectable absorption in the He I D_3 line.

3.13. V478 Lyr (HD 178450)

This BY Dra system is a single-lined spectroscopic binary with strong Ca II H & K emissions from the hot component (FFMCC) and a filled-in Hα absorption line (Fekel 1988).

The Hα spectrum of this system exhibits a strong filling-in absorption line (see Fig. 13). By subtracting the synthesized spectrum constructed with a G8V star we have obtained strong excess Hα emission, a small excess emission in the Na I D_1 and D_2 lines and a clear absorption in the He I D_3 line.

3.14. HK Lac (HD 209813)

HK Lac is a single-lined spectroscopic binary (F1V/K0III) with very strong Ca II H & K emissions, the Hϵ line in emission and an important excess Hα emission (FFMCC; Montes et al. 1995a).

This system shows a very variable Hα profile (from filled-in absorption to moderate emission) and flares (see Catalano & Frasca 1994). However, in our six Hα spectra taken in three consecutive nights, with orbital phases from 0.067 to 0.153, we always observe filled-in absorption line with small night to night variations in the excess Hα emission from the cool component. In Fig. 14 a spectrum of each night is showed.

The observed spectra are well matched using a K0III as reference star. The subtracted spectra show an important excess emission in the Na I D_1 and D_2 lines and a clear absorption in the He I D_3 line.

3.15. AR Lac (HD 210334)

The total eclipsing binary AR Lac is one of the best studied RS CVn systems. Both components of the system (G2IV/K0IV) are active (CABS), however, due to the orbital phase, in our previous Ca II H & K and Hα observations (FFMCC) it was not possible to separate the contribution from each component.

We analyse here Hα observations of this system at three orbital phases. In Fig. 15 we have superimposed to each spectrum the corresponding geometrical position of

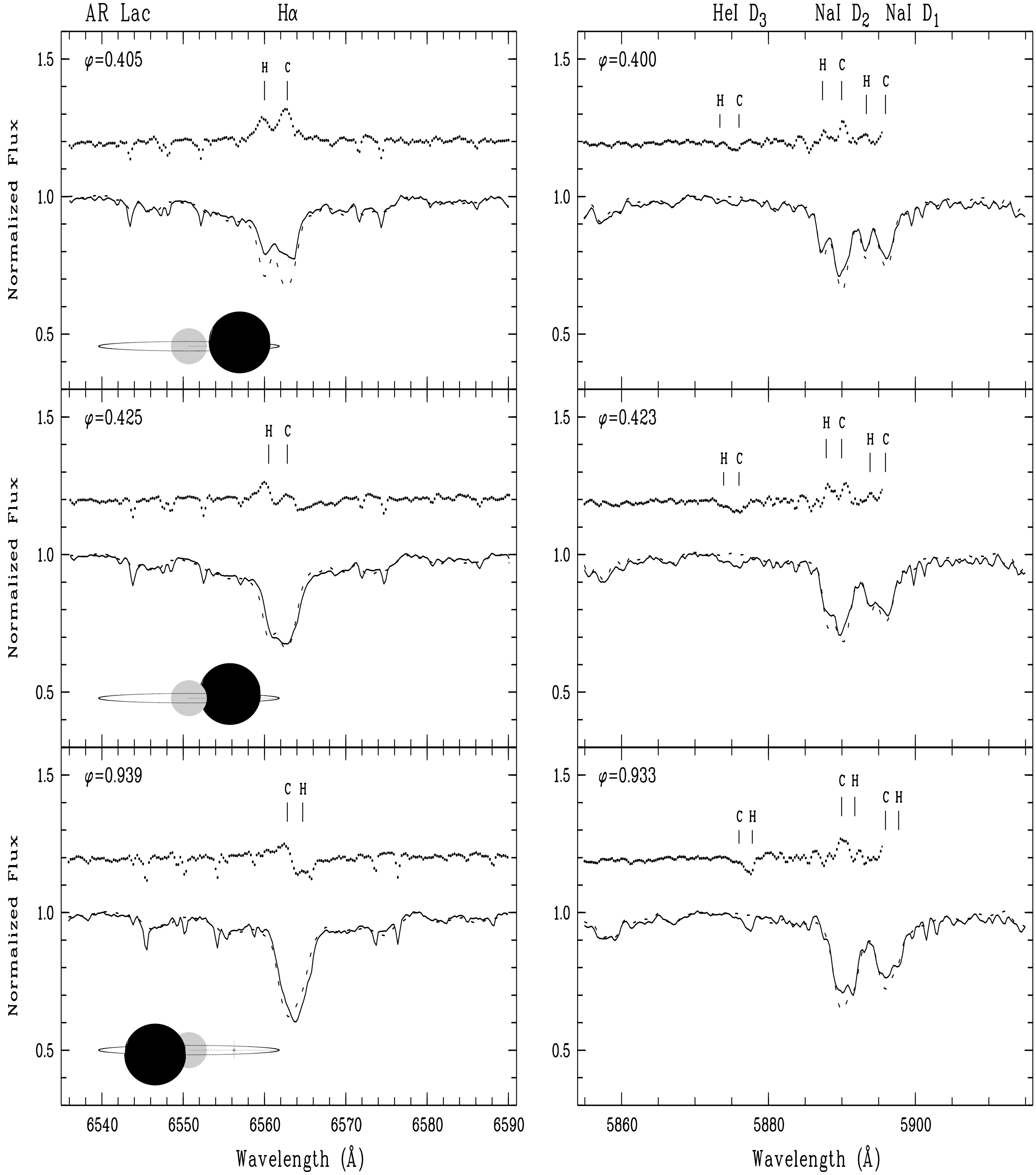

Fig. 15. Hα, Na I D_1, D_2, and He I D_3 spectra of AR Lac

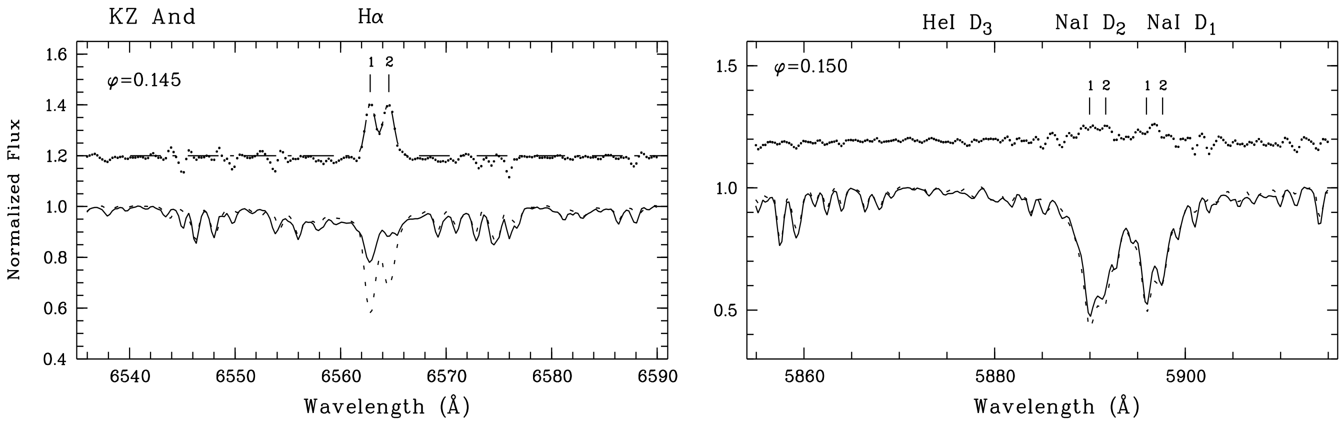

Fig. 16. Hα, Na I D_1, D_2, and He I D_3 spectra of KZ And

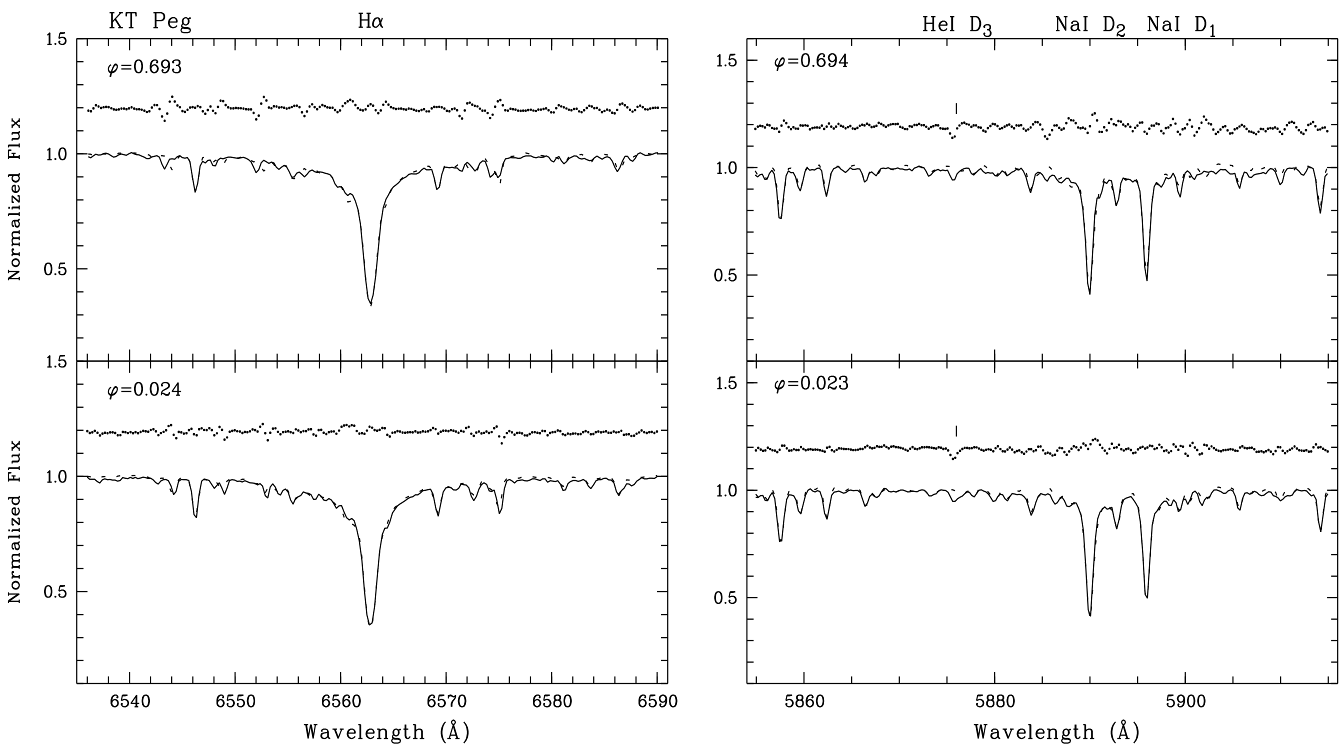

Fig. 17. Hα, Na I D_1, D_2, and He I D_3 spectra of KT Peg

the cool and hot components. At orbital phase 0.405 there is not eclipse and the subtracted spectrum exhibits excess Hα emission from both components, being a slightly larger that corresponding to the cool one. At phase 0.425 the hot component hides a 4% of the cool one and the excess emission obtained is now slightly larger in the hot component. This change in the excess emission observed in both components could be attributed to the hot component hiding of prominence-like material or other active regions responsible for the Hα emission of the cool component.

In the observation at the orbital phase 0.939, when a 33% of the hot component is hidden by the cool component, we detect an excess Hα absorption located at the wavelength position corresponding to the hot component. This excess absorption indicates the presence of prominence-like extended material seen off the limb of the cool component that absorbs the photospheric continuum radiation of the star behind. Similar prominence-like structures have been found in other eclipsing RS CVn systems (see Hall & Ramsey 1992) and recently, Siarkowski et al. (1996) have found geometrically extended structures in the corona of AR Lac.

At these three orbital phases the Na I D_1 and D_2 lines also present excess emissions from both components and

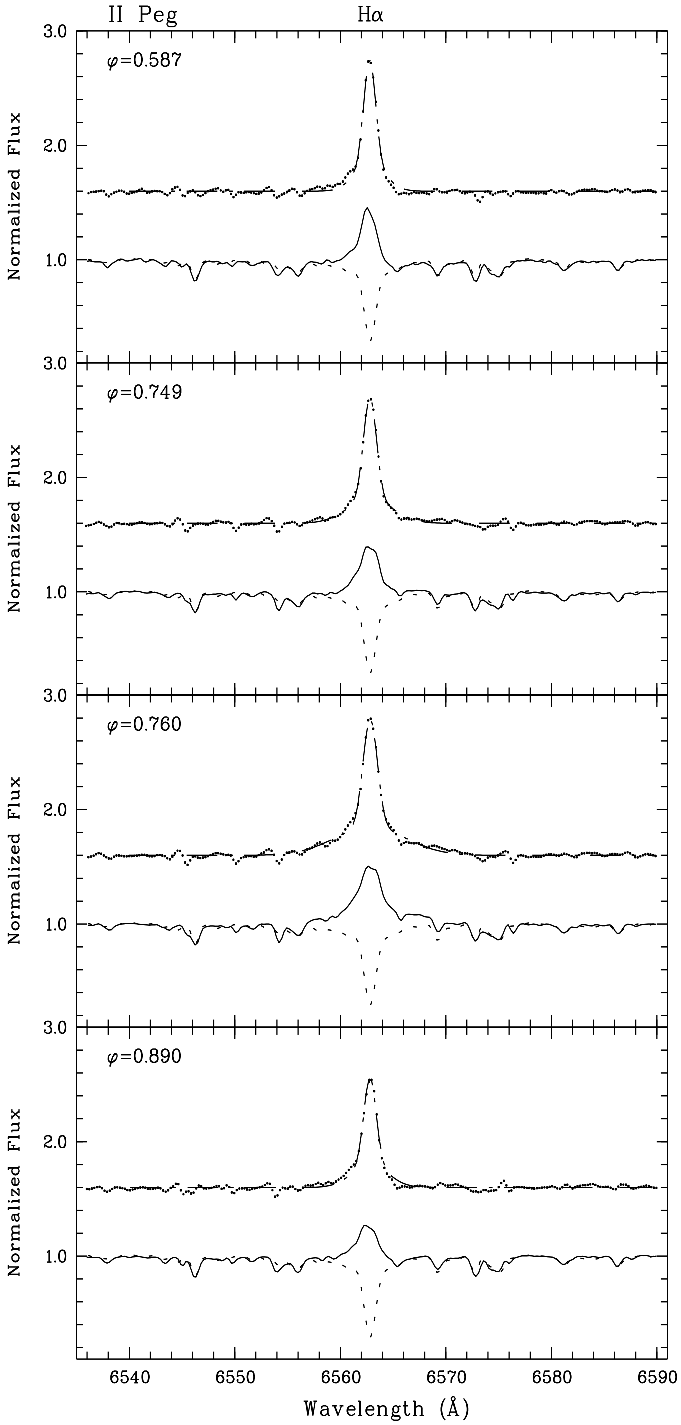

Fig. 18. Hα, Na I D_1, D_2, and He I D_3 spectra of II Peg

the He I D_3 shows absorption features in the subtracted spectra. At orbital phase 0.933 the He I D_3 line presents a large excess absorption at the wavelength position corresponding to the hot component, which could also be attributed to the prominence-like material.

3.16. KZ And (HD 218738)

KZ And is the component B of the visual pair ADS 16557, and is a double-lined spectroscopic binary with spectral types dK2/dK2. This system presents Ca II H & K and Hϵ emissions and excess Hβ emission from both components (FFMCC, Montes et al. 1995c,d).

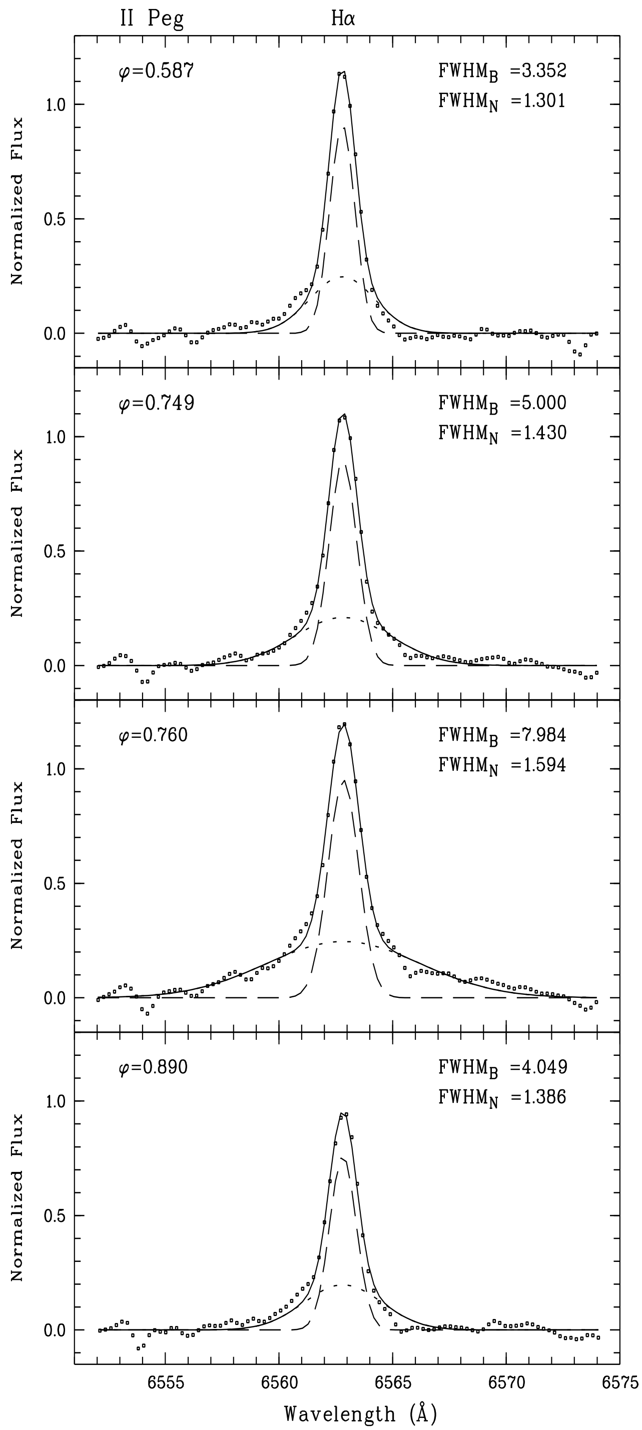

Fig. 19. Subtracted Hα profiles of II Peg at different orbital phases (dotted line). We have superposed the two Gaussian components fit (solid-line). The sort-dashed-line represents the broad component and the large-dashed-line the narrow one

By applying the spectral subtraction technique we have found that also both components present excess emission in the Hα line and in the in the Na I D_1 and D_2 lines, with very similar intensities (see Fig. 16). The He I D_3 line is not present in the subtracted spectrum. The synthesized spectrum has been constructed with two K2V stars and with a contribution of each component to the total continuum of 0.58/0.42.

3.17. KT Peg (HD 222317)

This system is a double-lined spectroscopic binary (G5V/K6V) with small Ca II H & K emissions from both components (Montes et al. 1995c).

We analyse here two spectra at the orbital phases 0.693 and 0.024 (see Fig. 17). We have constructed the synthesized spectrum with two reference stars of spectral types G2IV and K3V taking into account that the hot component has the larger contribution to the continuum. In both subtracted spectra no detectable excess emission is observed in the Hα line nor in the Na I D_1 and D_2 lines. The He I D_3 line appears in absorption.

3.18. II Peg (HD 224085)

This is a single-lined spectroscopic binary (K2 − 3V − IV) with strong Ca II H & K emission lines and variable Hα emission above the continuum. We have reported a strong excess emission in the Hβ line (Montes et al. 1995d).

We present here eight spectra of this system taken in three consecutive nights and with orbital phases ranging from 0.58 to 0.91. The strong Hα emission present in the subtracted spectra in all the phases shows remarkable night to night changes (see Fig. 18). In the second night the spectrum at orbital phase 0.760 shows a remarkable excess Hα emission enhancement with regard to the other phases, which is much more noticeable in comparison with the spectra of the first and third nights. The excess Hα emission EW increases in a factor of 1.9 in an interval of 1 day. This fact suggests that we have detected a flare since enhancements of this amount during flares are typical of chromospheric emission lines (Simon et al. 1980; Catalano & Frasca 1994) and has also been observed by us in the flare detected in UX Ari (Montes et al. 1996b).

The He I D_3 line appears in emission in the observed spectrum only at orbital phase 0.760 (see Fig. 18) corresponding to the increase of the emission observed in the Hα line. This fact supports the detection of a flare-like event, since in the Sun the He I D_3 line appears as absorption in plage and weak flares and as emission in strong flares (Zirin 1988). At the other orbital phases of the first and second night an small emission in He I D_3 is also present in the subtracted spectrum. However, in the third night where the Hα *EW* present the lower values the He I D_3 emission is not observed.

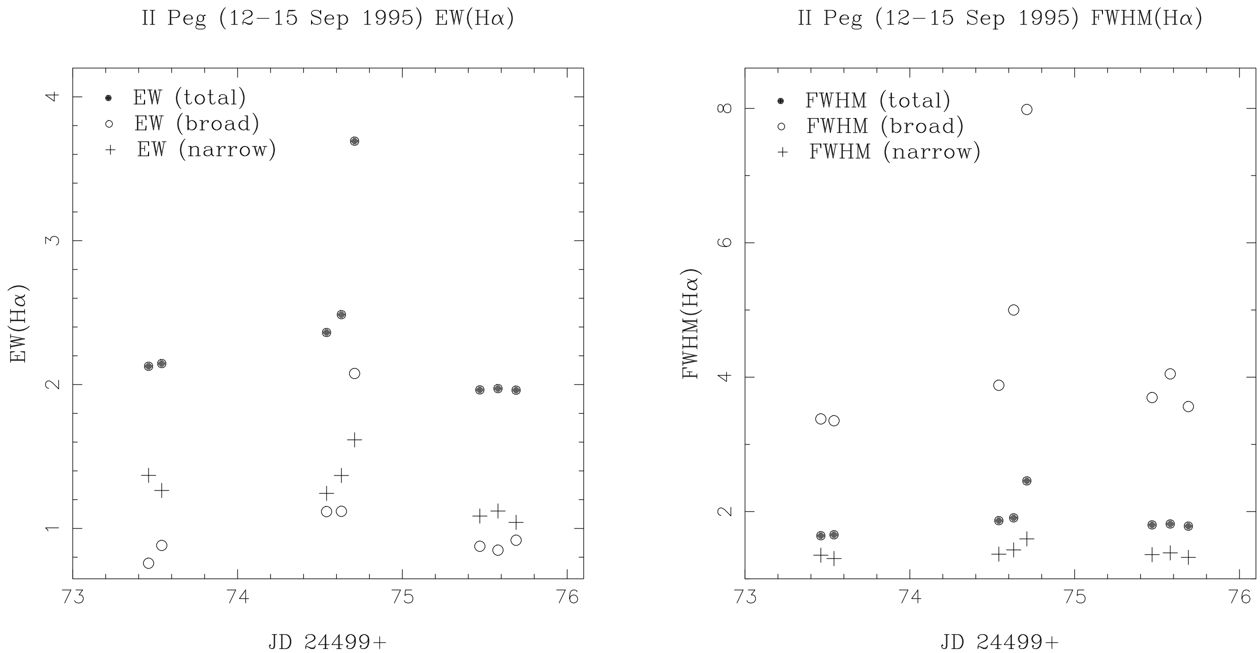

Fig. 20. Changes in the $EW(\mathrm{H}\alpha)$ and $FWHM(\mathrm{H}\alpha)$ of II Peg from 12-15 September 1995. Note the different behaviour of the broad and narrow components

The subtracted spectra show that the Hα profile presents broad wings, which are much more remarkable in the flare spectrum. In Fig. 19 we have represented the subtracted spectrum at phases 0.587, 0.749, 0.760 and 0.890 and the corresponding narrow and broad components used to perform the two-component Gaussian fit.

The changes in the $EW(\mathrm{H}\alpha)$ and $FWHM(\mathrm{H}\alpha)$ of the total subtracted spectra and of the corresponding narrow and broad components during the three nights can be seen in Fig. 20. Note the strong change in the $FWHM$ of the broad component during the flare.

4. Discussion

4.1. The excess Hα emission

The inspection of the subtracted Hα spectra shows that in some stars the emission line profile has very broad wings, and is not well matched using a single-Gaussian fit. These profiles have therefore been fitted using two Gaussian components: a narrow component having a $FWHM$ of 45–90 km s^{-1} and a broad component with a $FWHM$ ranging from 133 to 470 km s^{-1}. In Table 4 we list the parameters (I, $FWHM$, EW) of the broad and narrow components. As can be seen in this table the average contribution of the broad component to the total EW of the line ranges from 35% in AR Psc to 77% in V711 Tau. We have observed this behaviour in the chromospheric Hα line only in the most active systems of the sample, the stars with intense Hα emission above the continuum (AR Psc, XX Tri, UX Ari, V711 Tau (Fig. 6), II Peg (Fig. 19)) and also in systems with important excess Hα emission (MM Her, V815 Her, HK Lac). Furthermore, a revision of the Hα spectra of a large sample of chromospherically active binaries previously analysed by us (Montes et al. 1995a,b) indicates that the very active systems DM UMa and VV Mon also have broad components and that some systems also studied in this paper (V711 Tau, V815 Her, HK Lac) exhibit this behaviour at different epochs.

This parameterization of the subtracted Hα profile using a narrow and a broad component have been only reported until now for the RS CVn system DM UMa by Hatzes (1995) who suggests that the broad component could result from large-scale motions or winds in the chromosphere. Similar broad components have also been found in several transition region lines of the dM0e star AU Mic and the RS CVn systems Capella and V711 Tau using high-resolution UV observations obtained with the HST's GHRS (Linsky & Wood 1994; Linsky et al. 1995; Wood et al. 1996; Dempsey et al. 1996b,c; Robinson et al. 1996). The broad components in the transition region lines are interpreted by Linsky & Wood (1994) as arising from microflaring, because these broad profiles are reminiscent of the broad profiles observed in solar transition region explosive events, which are thought to be associated with emerging magnetic flux regions where field reconnection occurs.

The microflares are frequent, short-duration, energetically weak disturbances, i.e. they are the low-energy extension of flares, and therefore have large-scale motions

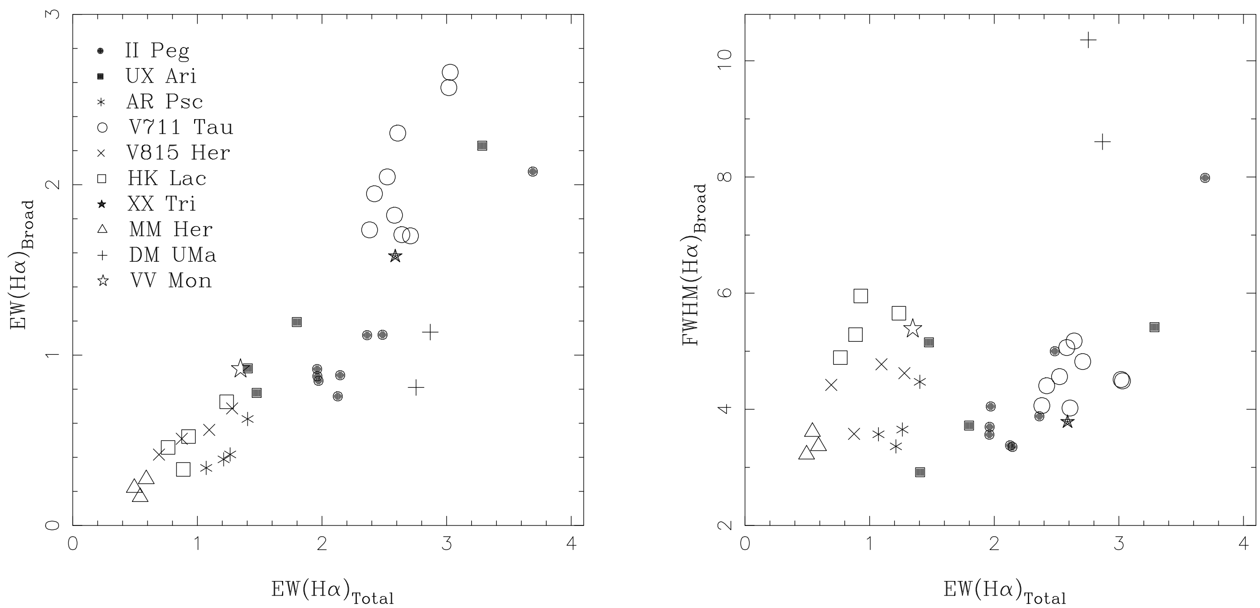

Fig. 21. $EW(\mathrm{H}\alpha)$ (left-panel) and $FWHM(\mathrm{H}\alpha)$ (right-panel) of the broad component versus the total $EW(\mathrm{H}\alpha)$. We have used different symbols for each star

associated that could explain the broad wings observed in these lines. The microflaring activity could occur not only in the transition region but also in the chromosphere of very active stars as indicates the detection of broad components in the chromospheric Mg II h & k lines of V711 Tau (Wood et al. 1996) but not in the chromospheric lines of the less active star Capella (Linsky et al. 1995).

Our detection of broad wings in the chromospheric Hα line of the most active systems of our sample allows us to conclude that microflaring occurs also in the chromosphere and that it is much more important in extremely active stars. Furthermore, within the group of stars that present this phenomenon a correlation between the contribution of the broad components and the degree of stellar activity seems to be present, as can be seen in Fig. 21 left-panel where we have plotted for each star the EW of the broad component versus the total excess Hα EW. This correlation was also noted by Wood et al. (1996) when compared the dominant broad component of V711 Tau with the smaller broad component of the less active stars AU Mic and Capella.

On the other hand, when we plot the $FWHM$ of the broad component versus the total Hα EW (Fig. 21 right-panel) a general trend is not observed. However, in this case the relation appears for individual star, i.e. there is an increase in the FWHM when the activity level increases, which is consistent with the hypothesis that microflaring is responsible for the broad component emission.

We have also found that the larger changes in the excess Hα emission in the stars analyzed appear to occur predominantly in the broad component, as have been already noted in the case of DM UMa by Hatzes (1995). An extreme case of this behaviour is the strong change in the broad component that occurs during the flares detected in UX Ari and II Peg (see Figs. 20 and 21). Since large scale mass motions do occur in solar flares, a large flare in these two systems may explain the increase of the Hα emission and the very broad wings observed in these spectra.

4.1.1. The He I D_3 line

The He I D_3 λ5876 and He I λ10830 triplets are known to be activity indicators in the Sun and late type stars (Zirin 1988; Shcherbakov et al. 1996). In the Sun, the He I D_3 line appears like an absorption feature cospatial with plages (Landman 1981), and it almost disappears when we look at the solar disk. This feature is also seen in absorption in surges, eruptive prominences, and weaker flares, whereas in emission in more intense flares (Zirin 1988).

The He I D_3 line is formed at middle chromosphere, and its correlation with X-ray flux and Ca II H & K lines suggests that the fractional area of the stellar disk covered by plages may be a key factor in the formation of D_3 (Danks & Lambert 1985). Moreover it has been observed a slight rotational modulation in κ Cet (Lambert & O'Brien 1983) and χ^1 Ori (Danks & Lambert 1985).

Table 4. Parameters of the broad and narrow Gaussian components used in the fit of the Hα subtracted spectra of the stars analysed in this paper and in V711 Tau, V815 Her, HK Lac, DM UMa, and VV Mon from our previous observations (Montes et al. 1995a,b)

Name	φ	Hα broad component				Hα narrow component			
		I	$FWHM$ (Å)	EW_B (Å)	EW_B/EW_T (%)	I	$FWHM$ (Å)	EW_N (Å)	EW_N/EW_T (%)
AR Psc	0.373	0.089	3.570	0.338	31.6	0.541	1.272	0.732	68.3
	0.443	0.132	4.473	0.625	44.5	0.534	1.358	0.772	55.0
	0.519	0.108	3.362	0.388	32.0	0.587	1.319	0.823	68.0
	0.524	0.107	3.652	0.417	33.0	0.603	1.316	0.845	67.0
XX Tri	0.401	0.392	3.785	1.581	60.8	0.712	1.132	1.007	38.7
UX Ari	0.419	0.302	3.720	1.194	66.4	0.431	1.317	0.605	33.6
	0.438	0.297	2.917	0.922	65.6	0.344	1.316	0.483	34.4
	0.576	0.145	5.153	0.778	50.8	0.468	1.512	0.753	49.2
	0.736	0.405	**5.414**	2.229	67.8	0.580	1.723	1.069	32.4
V711 Tau (1995)	0.922	0.335	4.822	1.700	62.7	0.502	1.852	0.990	36.5
	0.261	0.425	4.563	2.046	81.1	0.344	1.254	0.459	18.2
	0.280	0.417	4.406	1.947	80.4	0.344	1.265	0.463	19.1
	0.606	0.318	5.176	1.707	64.6	0.509	1.635	0.887	33.6
	0.641	0.402	4.063	1.735	72.8	0.406	1.486	0.642	27.0
V711 Tau (1992)	0.130	0.546	4.022	2.303	88.3	0.234	1.226	0.305	11.7
V711 Tau (1986)	0.200	0.570	4.489	2.660	87.8	0.251	1.381	0.369	12.2
	0.260	0.576	4.513	2.570	85.2	0.311	1.486	0.448	14.8
V711 Tau (1988)	0.880	0.362	5.063	1.821	70.5	0.410	1.743	0.761	29.5
MM Her	0.498	0.076	3.367	0.272	46.1	0.248	1.203	0.318	53.9
	0.630	0.044	3.612	0.167	30.9	0.274	1.283	0.374	69.1
	0.745	0.064	3.222	0.221	44.7	0.217	1.180	0.273	55.3
V815 Her (1995)	0.978	0.142	4.622	0.687	53.7	0.397	1.377	0.582	45.5
	0.520	0.134	3.577	0.509	58.2	0.267	1.288	0.366	41.8
	0.099	0.113	4.775	0.561	51.2	0.334	1.467	0.521	47.6
V815 Her (1989)	0.520	0.092	4.420	0.416	60.1	0.200	1.294	0.276	39.9
HK Lac (1995)	0.067	0.089	4.890	0.458	59.9	0.291	0.991	0.307	40.1
	0.110	0.095	5.286	0.515	58.1	0.329	1.065	0.373	42.0
	0.149	0.089	5.951	0.522	56.2	0.339	1.129	0.408	43.9
HK Lac (1989)	0.100	0.142	5.654	0.726	58.8	0.346	1.384	0.509	41.2
II Peg	0.575	0.211	3.379	0.758	35.6	0.952	1.351	1.369	64.4
	0.587	0.247	3.352	0.882	41.1	0.913	1.301	1.264	58.9
	0.735	0.271	3.880	1.118	47.3	0.856	1.366	1.244	52.7
	0.749	0.210	5.000	1.119	45.0	0.898	1.430	1.368	55.0
	0.760	0.245	**7.984**	2.077	56.3	0.952	1.594	1.616	43.7
	0.874	0.223	3.697	0.876	44.6	0.750	1.359	1.086	55.3
	0.890	0.197	4.049	0.849	43.1	0.761	1.386	1.121	56.8
	0.907	0.242	3.563	0.918	46.8	0.743	1.319	1.042	53.1
DM UMa	0.400	0.207	10.36	0.810	27.8	0.999	1.971	2.107	72.2
	0.530	0.246	8.607	1.135	38.0	0.918	1.893	1.850	62.0
VV Mon	0.710	0.177	5.382	0.918	68.2	0.252	1.596	0.428	31.8

Historically, there have been basically two models to explain the line formation of He I D_3: (i) Zirin (1975) suggested that He I triplet levels were populated by overphotoionisation of the He I atoms by EUV and X-ray radiation, and subsequent radiative recombinations and cascade. (ii) Wolff et al. (1985) argued that collisional excitation and ionization in the chromosphere contributed also to the He I D_3 formation, and not only the EUV and X-ray radiation from the corona. However, the most recent models (Andretta & Giampapa 1995; Lanzafame & Byrne 1995) seem to indicate that the primary mechanism in the formation of the He I triplets is the collisional excitation and ionization (followed by recombination cascade) by electron impact.

The He I D_3 line usually appears, in stars, in absorption, but sometimes is in emission. There are two possible reasons: (i) Temperature and/or electronic density conditions are higher than ordinary, like may occur in flares (Zirin 1988; Andretta & Giampapa 1995; Lanzafame & Byrne 1995). (ii) As it has been seen in He I λ10830, depending on the position of the emitting region in the disk or off the limb, the He I D_3 line would appear in absorption or emission. Since the He I λ10830 is formed in emitting regions located at some distance from the stellar photosphere, when the emitting region is seen in projection against the stellar disk, He I λ10830 line appears in absorption, and when the emitting region is observed off the stellar limb, the line is in emission (Simon et al. 1982; Wolff & Heasley 1984). These conclusions could extend to the case of He I D_3, since it is produced at the same region that He I λ10830.

The He I D_3 line has been studied only in some chromospherically active binaries as II Peg (Huenemoerder & Ramsey 1987; Huenemoerder et al. 1990), DM UMa (Hatzes 1995), ER Vul (Gunn & Doyle 1997) and GK Hya (Gunn et al. 1997). The observation of emission in the He I D_3 line supports the detection of flare like events as in the case of II Peg (Huenemoerder & Ramsey 1987) and the weak-lined T Tauri star V410 Tau (Welty & Ramsey 1997).

In our spectra the He I D_3 line has been found in emission only during the flares of UX Ari and II Peg. We wish to emphasize that the detection of He I D_3 in emission in the RS CVn systems seems to occur at orbital phases near to the quadrature. In our observations we have detected He I D_3 in emission at orbital phase 0.74 in UX Ari (Montes et al. 1996b) and at 0.76 in II Peg. This line has been also observed in emission at orbital phases 0.22, 0.26, 0.77 in II Peg by Huenemoerder & Ramsey (1987) and Huenemoerder et al. (1990). Probably we are observing a flare off the limb, i.e. when the plage regions are near the limb (the active regions are preferably in the opposite faces of the stars), which is the most favourable situation to see an off the limb flare. But we cannot distinguish whether the emission is only due to the existence of the flare, or it is favoured by the relative position on the star.

The application of the spectral subtraction to our sample reveals that the He I D_3 line appears as an absorption feature more frequently in giants than in dwarfs. Three out of five giants observed show clear absorptions (BD Cet, V1149 Ori and HK Lac) and two of them exhibit a possible absorption (AY Cet and XX Tri), while among IV and V luminosity class stars there are only two plain absorptions. Various authors seem to point out a more frequent presence of He I λ10830 and λ5876 triplets in giants and supergiants than in dwarfs (Simon et al. 1982; Zirin 1982; Wolff & Heasley 1984).

Zirin (1982) observed He I λ10830 usually in absorption, but sometimes it appears in emission, especially in giant and supergiants, with a P Cygni form, and he attributes it to a mass-ejection phenomenon (see also O'Brien & Lambert 1986). Simon et al. (1982) saw that none of the single red giants, in their sample, having strong λ10830 absorption or emission has prominent transition region emission lines or soft X-ray emission, and they proposed a scattering process-like responsible for the λ10830 line formation. Smith (1983) attributed a larger intensity in λ10830 line for giants and supergiants to the most efficient ionization by EUV and X-ray radiation in atmospheres of coronally active giants. Other authors say that λ10830 line is sometimes produced by the propagation of acoustic shock waves, or that He I λ10830 transition represents a wind diagnostic. Some of the above proposed mechanisms could also be applied to the He I D_3 line.

4.1.2. The Na I D_1 and D_2 lines

The Na I D_1 and D_2 lines are collisionally-controlled in the atmospheres of late-type stars and are formed in the lower chromosphere. So, the detection of filled - in absorption in the D_1 and D_2 lines may provide information about chromospheric emission. (see the recent models of these lines for M dwarfs stars by Andretta et al. 1997).

In the Sun, Barrado et al. (1995) and Barrado (1996) have found changes in the *EW* of Na I lines in spectra taken at different regions over the solar surface, and a relation with the filled-in absorption Hα that might indicate that there is a non-radiative effect in the formation of these lines.

In other stars the D_1 and D_2 lines have been observed in emission or as a filled-in in very active red dwarf flare stars (Pettersen et al. 1984; Pettersen 1989). However, no systematic study of these lines has been performed in stars with different levels of activity, and in chromospherically active binaries only the negative and uncertain detection of filled-in in the few active binaries ER Vul and GK Hya, respectively, has been reported in the recent studies of Gunn & Doyle (1997) and Gunn et al. (1997).

The application of the spectral subtraction technique in these lines is more difficult that in the Hα line, because their wings are very sensitive to the effective temperature, mainly in latter spectral types. Therefore, small differences in spectral type, not appreciated in the Hα line, produce significant changes of the subtracted spectra in the wings of the Na I lines. Moreover, in this spectral region there is a large number of telluric lines, and in the spectra of some stars interstellar Na I could be present. However, the distances of the majority of the stars is lower than 50 pc and the effect of the interstellar Na I is negligible.

In spite of this problems, some conclusions can be drawn. In the chromospherically active binaries analysed here, the spectral subtraction reveals that the core of the Na I D_1 and D_2 lines are filled-in by chromospheric emission in the more active star of the sample (the star with Hα emission above the continuum, and with larger excess Hα emission *EW*). The stars with only a small or without excess Hα emission as BD Cet, AY Cet, V1149 Ori and KT Peg do not exhibit excess emission in the Na I lines. Moreover, the excess D_1 and D_2 emissions obtained are larger in the systems with larger excess Hα emission, and also increase in the flares observed in UX Ari and II Peg. In short, we can conclude that the filled-in of the core of the Na I D_1 and D_2 lines could be used as a chromospheric activity indicator.

5. Conclusions

In this paper we have analysed, using the spectral subtraction technique, simultaneous Hα, Na I D_1, D_2, and He I D_3

spectroscopic observations of 18 chromospherically active binary systems.

We have found excess Hα in all the systems, except KT Peg which have also small emission in the Ca II H & K lines. The subtracted Hα profile of the more active stars of the sample (Hα in emission above the continuum) has very broad wings, and is well matched using a two-components Gaussian fit (narrow and broad). The broad component is primarily responsible for the observed variations of the profile, and its contribution to the total EW increases with the degree of activity. So, we have interpreted this broad component emission as arising from microflaring activity that take place in the chromosphere of these very active stars.

The Hα observation of the eclipsing binary system AR Lac at orbital phase 0.939, when a 0.33 fraction of the hot component is hidden by the cool component, allowed us to detect the presence of prominence-like extended material seen off the limb of the cool component through the detection of excess Hα absorption located at the wavelength position corresponding to the hot component. A small excess absorption in the He I D_3 line is also present at this orbital phase.

We reported the detection of an optical flare in the systems UX Ari and II Peg through the presence of the He I D_3 in emission in coincidence with the enhancement of the Hα emission.

We have found the He I D_3 in emission only in the two above mentioned flares, and as an absorption feature in the subtracted spectra of a large number of giant stars of the sample.

The application of the spectral subtraction technique reveals that the core of the Na I D_1 and D_2 lines are also filled-in by chromospheric emission in the more active star of the sample. The stars with only a small excess Hα emission do not exhibit excess emission in the Na I lines.

Acknowledgements. This work has been supported by the Universidad Complutense de Madrid and the Spanish Dirección General de Investigación Científica y Técnica (DGICYT) under grant PB94-0263. We would like to thank the referee S. Catalano for suggesting several improvements and clarifications.

References

Andretta V., Giampapa M.S., 1995, ApJ 439, 405
Andretta V., Doyle J.G., Byrne P.B., 1997, A&A 322, 266
Basri G., Wilcots E., Stout N., 1989, PASP 101, 528
Barrado D., De Castro E., García López R.J., Sánchez Almeida J., Montesinos B., 1995, in: Stellar Surface Structure, IAU Symp. 176, Poster Proceedings, Strassmeier K. (ed.) p. 123
Barrado D., 1996, Th. Doctoral, Universidad Complutense de Madrid
Bidelman W.P., McConnell D.J., 1973, AJ 78, 687
Bopp B.W., Fekel F., Aufdenberg J.P. Dempsey R., Dadonas V., 1993, AJ 106, 2502
Catalano S., Frasca A., 1994, 287, 575
Danks A.C., Lambert D.L., 1985, A&A 148, 293
Dempsey R.C., Neff J., O'Neal D., Olah K., 1996a, AJ 111, 1356
Dempsey R.C., Neff J., Linsky J.L., Brown A., 1996b, IAU Symp. 176, Strassmeier K.G. & Linsky J.L. (eds.) Stellar Surface Structure, p. 411
Dempsey R.C., Neff J., Thorpe M.J., et al., 1996c, ApJ 470, 1172
Fekel F.C., Moffett T.J., Henry G.W., 1986, ApJS 60, 551
Fekel F.C., 1988, AJ 95, 215
Fekel F.C., 1996, AJ 112, 269
Fernández-Figueroa M.J., Montes D., De Castro E., Cornide M., 1994, ApJS 90, 433 (FFMCC)
Gunn A.G., Doyle J.G., 1997, A&A 318, 60
Gunn A.G., Doyle J.G., Houdebine E.R., 1997, A&A 319, 211
Hall J.C., Ramsey L.W., 1992, AJ 104, 1942
Hall J.C., 1996, PASP 108, 313
Hampton M., Henry G.W., Eaton J.A., Nolthenius R.A., Hall D.S., 1996, PASP 108, 68
Hatzes A.P., 1995, AJ 109, 350
Huenemoerder D.P., Ramsey L.W., 1987, ApJ 319, 392
Huenemoerder D.P., Ramsey L.W., Buzasi D.L., 1990, Cool star stellar systems and the Sun, Sixth Cambridge Workshop., Wallerstein G. (ed.), ASP Conf. Ser. 9, 236
Lambert D.L., O'Brien G.T., 1983, A&A 128, 110
Landman D.A., 1981, ApJ 244, 345
Lanzafame A.C., Byrne P.B., 1995, A&A 303, 155
Lázaro C., Arévalo M.J., 1997, AJ 113, 2283
Linsky J.L., Wood B.E., 1994, ApJ 430, 342
Linsky J.L., Wood B.E., Judge P., Brown A., Andrulis C., Ayres T.R., 1995 ApJ 442, 381
Montes D., De Castro E., Cornide M., Fernández-Figueroa M.J., 1994, in: Cool Stars, Stellar Systems, and the Sun, Eighth Cambridge Workshop, Caillault J.P. (ed.) ASP Conf. Ser. 64, 444
Montes D., Fernández-Figueroa M.J., De Castro E., Cornide M., 1995a, A&A 294, 165
Montes D., Fernández-Figueroa M.J., De Castro E., Cornide M., 1995b, A&AS 109, 135
Montes D., De Castro E., Fernández-Figueroa M.J., Cornide M., 1995c, A&AS 114, 287
Montes D., Fernández-Figueroa M.J., De Castro E., Cornide M., 1995d, Stellar Surface Structure, IAU Symp 176, Poster Proceedings, Strassmeier K. (ed) p. 167
Montes D., Fernández-Figueroa M.J., Cornide M., De Castro E., 1996a, A&A 312, 221
Montes D., Sanz-Forcada J., Fernández-Figueroa M.J., Lorente R., 1996b, A&A 310, L29
Montes D., Martín E.L., Fernández-Figueroa M.J., Cornide M., De Castro E., 1997, A&AS 123, 473
O'Brien G.T., Lambert D.L., 1986, ApJS 62, 899
Pasquini L., Pallavicini R., 1991, A&A 251, 199
Pettersen B.R., Evans D.S., Coleman L.A., 1984, ApJ 282, 214
Pettersen B.R., 1989, A&A 209, 279
Robinson R.D., Airapetian V.S., Maran S.P., Carpenter K.G., 1996, ApJ 469, 872
Shcherbakov A.G., Shcherbakova Z.A., Tuominen I., Jetsu L., 1996, A&A 309, 655
Simon T., Linsky J.L., Schiffer F.H., 1980, ApJ 239, 911
Simon T., Linsky J.L., Stencel R.E., 1982, ApJ 257, 225

Siarkowski M., Preś P., Drake S.A., White N.E., Singh K.P., 1996, ApJ 473, 470
Smith M.A., 1983, AJ 88, 1031
Strassmeier K.G., Fekel F.C., Bopp B.W., Dempsey R.C., Henry G.W., 1990, ApJS 72, 191
Strassmeier K.G., Hall D.S., Fekel F.C., Scheck M., 1993, A&AS 100, 173 (CABS)
Welty A.D., Ramsey L.W., 1997, AJ (in press)
Wolff S.C., Heasley J.N., 1984, PASP 96, 231
Wolff S.C., Heasley J.N., Varsik J., 1985, PASP 97, 707
Wood B.E., Harper G.M., Linsky J.L., Dempsey R.C., 1996, ApJ 458, 761
Xuefu L., Huisong T., 1984, Inf. Bull. Var. Stars No. 2606
Zirin H., 1975, ApJ 199, L163
Zirin H., 1982, ApJ 260, 655
Zirin H., 1988, in Astrophysics of the Sun. Cambridge University Press